MARINE AEROSOL PHYSICAL PROPERTIES AND INFLUENCES BY METEOROLOGY IN THE NORTH ATLANTIC OCEAN

by

Nicole Chisholm

Submitted in partial fulfilment of the requirements
for the degree of Master of Science

Dalhousie University
Halifax, Nova Scotia
August 2020

Table of Contents

List of Tables

List of Figures

Abstract

Marine aerosols play an important role in earth's climate, but their effects remain highly uncertain due to a poor understanding of their sources, properties, and atmospheric processing, partly due to limited measurements. The Coastal-Fog (C-FOG) study investigated the processes controlling the formation and properties of fog in the North Atlantic Ocean. As part of this study, aerosol particle size distributions and chemical composition were measured off the shore of the northeastern United States and Atlantic Canada, and used to investigate the sources and processes affecting the observed aerosols. Processed marine air during the study was characterized by single and bi-modal aerosol size distributions. Aerosols in the port city of St. John's, Newfoundland reflected local emissions built up due to poor ventilation, whereas aerosols in Halifax, Nova Scotia were lower in concentration because the harbour is more spread out. Finally, two particle growth events were observed. The first event captured the appearance of 10 nm particles that grew to 30 nm over 4 h. These aerosols appeared to be newly formed in the upper portion of the boundary layer with influence from the free troposphere before subsiding to the surface. In the second event, 45 nm particles grew to 70 nm over 8 h. The growth of these aerosols was most likely due to the direct condensation of organic vapours emitted from boreal forests and/or the ocean. Our observations provide important insight into the processes affecting marine aerosols and highlight the crucial role of boundary layer meteorology.

List of Abbreviations and Symbols Used

θ	Potential temperature
κ	Hygroscopicity
μm	Micrometer
ACE	Aerosol Characterization Experiment
ACSM	Aerosol Chemical Speciation Monitor
APS	Aerodynamic Particle Sizer
a.s.l.	Above sea level
Br^-	Dissolved bromide ion
CCN	Cloud condensation nuclei
CCNC	Cloud Condensation Nuclei Counter
Cl^-	Dissolved chloride ion
cm	centimeter
CPC	Condensation Particle Counter
D_m	Mobility diameter
DMA	Differential Mobility Analyzer
DMS	Dimethyl sulfide
FT	Free troposphere
g	Gram
GFS	Global Forecast System
GPS	Global Positioning System
hPa	Hectopascal
HYSPLIT	Hybrid Single-Particle Lagrangian Integrated Trajectory
IPCC	Intergovernmental Panel on Climate Change
K	Kelvin
K^+	Dissolved potassium
kg	Kilogram
km	Kilometer
Li^+	Dissolved lithium

l.p.m.	Liters per minute
m	Meter
MBL	Marine Boundary Layer
mM	Millimolar
mm	Millimeter
$m\ s^{-1}$	Meters per second
MOUDI	Microorifice Uniform Deposit Impactor
MSA	Methylsulfonic acid
Na^{+}	Dissolved sodium
NAAMES	North Atlantic Aerosols and Marine Ecosystems Study
NaCl	Sodium chloride
NAM	North American Mesoscale Forecast System
NASA	National Aeronautics and Space Administration
NCEP	National Centers for Environmental Prediction
NH_4^+	Dissolved ammonium
NO_2^-	Dissolved nitrogen dioxide
NO_3^-	Nitrate
NO_x	Nitrogen oxides
NOAA	National Oceanic and Atmospheric Administration
P	Pressure
Pg	Petagram
PO_4^{3-}	Dissolved phosphate
ppt	Parts per trillion
pptv	Parts per trillion volume
q	Specific humidity
SMPS	Scanning Mobility Particle Sizer
SO_2	Sulfur dioxide
SO_4^{2-}	Dissolved sulfuric acid
T	Temperature
UTC	Coordinated Universal Time
V	Volts

VOCs	Volatile Organic Compounds
yr	Year

Acknowledgements

First, I would like to thank my supervisor, Dr. Rachel Chang, for all her help and guidance on this project. Without her this thesis would not have been possible. I would like to thank Dr. Betty Croft as well for her insight and interpretation of the events analyzed in this thesis. In addition, I would also like to thank: Dr. Charlotte Wainwright and Dr. Joe Hernando from University of Notre Dame for the use of their meteorology data gathered on the ship; Dr. Clive Dorman for his insight on the meteorology during the events analyzed; Dr. Trevor VandenBoer and Leyla Salehpoor from York University for providing the chemical analysis data from the MOUDI; Dr. Ian Folkins and Dr. Glen Lesins from Dalhousie University for acting as committee members. Finally, I would like to thank my friends and family for their encouragement and support throughout my academic career.

Chapter 1: Introduction

1.1 General Aerosol Background

Aerosols are small particles in the solid and liquid state that are suspended in air. They are present in the atmosphere all around the world and can have important impacts on health and climate. Aerosols can be emitted in a range of sizes from the nanometer to the micrometer range and can also form in the atmosphere from gaseous precursors under given conditions. Atmospheric aerosols exist in the two lowest levels of the atmosphere, the troposphere and the stratosphere, and can originate from both natural and anthropogenic sources (Seinfeld and Pandis 2016) with most of the aerosol mass residing in the troposphere (Jacob 1999).

The troposphere has many primary sources of aerosols such as marine, desert, forest, and anthropogenic and can take the form of sea spray, dust, smoke from biomass burning, and fossil fuels. These primary aerosols are particles that enter the atmosphere directly. Along with these primary sources, there are secondary sources of aerosols which are also formed in the troposphere, but through secondary production such as the formation from dimethylsulfide (DMS) oxidation products (Lovelock et al. 1972), volatile organic compounds (VOCs) (Ovadnevaite et al. 2014), and secondary sulfates and nitrates, as well as through transport from the stratosphere. Aerosols can be lost through different sinks such as dry deposition, wet deposition, coagulation with cloud droplets or rain, and scavenging by other aerosols. The aerosols in the stratosphere originate from aerosol and precursor gases transported from the troposphere as well as direct injections of volcanic ash aerosols (Kremser et al. 2016).

1.2 Atmospheric Aerosols

1.2.1 Processes Affecting Aerosols

Processes such as condensation of precursor gases and coagulation with other aerosols can grow existing aerosols in the atmosphere (Seinfeld and Pandis 2016) with some of these aerosols potentially becoming cloud condensation nuclei (CCN) and forming cloud droplets if the atmospheric conditions are suitable. Condensation and coagulation that occurs in the atmosphere modifies the aerosols and can therefore impact the aerosol's effect on atmospheric processes.

When the condensation sink is low due to the absence of existing particles, the secondary process called aerosol nucleation can occur. Figure 1.1 illustrates classical nucleation theory, where nucleation occurs when the gain rate of molecules combining to form an aerosol is greater than the loss rate of the molecules due to evaporation (Seinfeld and Pandis 2016). Molecules can cluster together and, depending on atmospheric conditions, these clusters will grow or evaporate. Once a cluster reaches a critical size, typically 1 nm, it is considered a nucleated aerosol and can contribute to the aerosol processes occurring in the atmosphere as well as participate in the growth of a CCN through condensation of components such as sulfates, ammonia, and VOCs, and through coagulation with other aerosols.

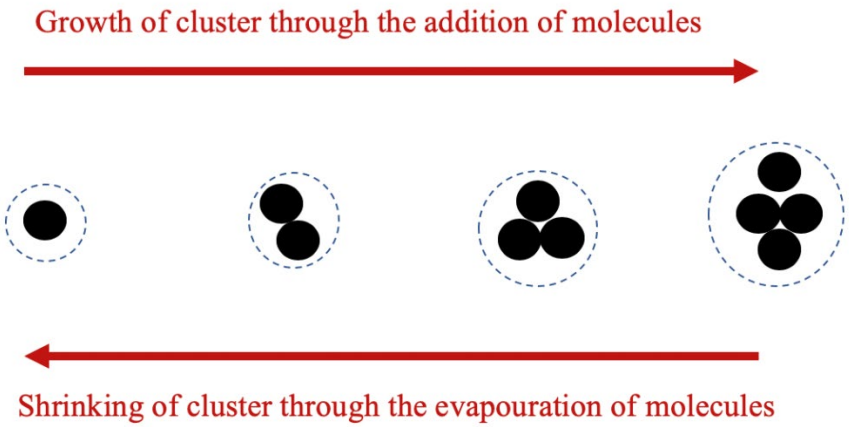

Figure 1.1: Nucleation process of atmospheric aerosols.

Nucleation can only occur in the atmosphere when certain conditions are met and the understanding of these conditions can provide better insight. Nucleation is usually favored when both temperature and condensation sinks are low in the atmosphere. Over the North Atlantic, this usually occurs in the free troposphere because of the low aerosol concentrations and cooler temperatures, but can also occur in the boundary layer during the late fall and winter months (Sanchez et al. 2018). Low particle concentrations do not usually occur in the boundary layer because of the constant emission of aerosol sources from the surface. These emitted aerosols will compete for the available precursor gases and prevent the nucleation of new aerosols because condensation will occur on an existing surface before creating a new one. Low temperatures are favourable for nucleation because condensation from gas to liquid phase is more likely to occur than evaporation. It has also been shown that conditions are more favorable for new particle formation after the passage of a cold front since it can clean out existing particles through precipitation and bring post frontal subsidence from the free troposphere and therefore newly formed small particles and their gaseous precursors (Bates et al. 1998).

Computer simulations have demonstrated that ternary nucleation can produce new particles when the particle number concentration is low, SO_2 is 20 to 50 pptv (Covert et al. 1992), and the ammonia concentration greater than 5 ppt (Croft et al. 2019; Pirjola et al. 2000). The atmospheric processes simulated in Covert et. al (1992), associated with ternary nucleation are adiabatic cooling and entrainment from the free troposphere, for which a conditionally unstable boundary layer is needed for mixing. The strongest nucleation was predicted for high entrainment rates (~30% free tropospheric air) into the marine boundary layer (Pirjola et al. 2000; David S. Covert et al. 1992).

In summary, the understanding of the nucleation of aerosols in the atmosphere will help to decrease the uncertainty in the sources of aerosols in the atmosphere as well as give insight on processes affecting the aerosols in the atmosphere. The accepted theory of nucleation is that it occurs in the free troposphere where the favourable conditions of low aerosol concentrations and high precursor gases are located. However, there have also been cases where nucleation can occur in the boundary layer if favourable conditions arise. The determination of the part of the atmosphere that nucleation occurs can provide a better understanding of aerosols and their atmospheric processes.

The R/V Hugh R. Sharp sailed along the east coast of Canada and the northeastern United States which varied from 39° to 48° latitude. This location is under the influence of the westerlies that flow from the west to east. These westerlies bring surface high- and low-pressure systems moving to the east which will in general transport air from the continent and moisture from the

south. This can influence growth, formation, and scavenging processes that occur in the marine boundary layer that affect the aerosol population.

High- and low-pressure systems affect the aerosol properties in multiple ways. For example, high pressure systems can entrain air from the free troposphere into the boundary layer, including aerosols from different sources and gases that could contribute to the chemistry, formation and growth of particles. Subsidence occurring from large scale subsidence, post-frontal subsidence, and the advection of anti-cyclonic systems (Covert et al. 1996) can lead to particle distributions with a smaller modal diameter (~25 nm). Aitken mode particles have been observed to be more numerous than accumulation mode particles when air subsides (minimal clouds and precipitation) (Covert et al. 1996).

Low pressure systems impact the interstitial aerosols in the atmosphere by cloud processing, which can grow the existing aerosols, and remove them through rainout. After rain events, particle concentrations have been observed to drop rapidly (Royalty et al. 2017) due to the scavenging of the more hygroscopic (sea salt) particles by activation and wet deposition (Sanchez et al. 2018). An increase in sulfate aerosol concentrations is also observed, most likely formed from secondary sulfate formation in cloud droplets (Ervens et al. 2011). Low pressure systems bringing cold fronts cause precipitation which can remove the accumulation mode particles through wet deposition, sometimes creating favorable conditions for nucleation (Bates et al. 1998). Frequent frontal passages also limit the residence time of Aitken mode particles at the mid-latitudes in the marine boundary layer to no more than three days (Bates et al. 1998; Quinn et al. 2017). This prevents the growth of those particles to the accumulation mode and

results in Aitken mode dominated distributions over time. Frontal passages can also bring Aitken and nucleation mode particles from the free troposphere to the marine boundary layer through subsidence around venting cumulus clouds (Covert et al. 1996; Bates et al. 1998).

The meteorology tracers of pressure, temperature, potential temperature, and specific humidity can be used to determine the level of the atmosphere the air parcel originated from by examining the atmospheric conditions at different levels. The observed pressure over time can indicate if subsidence was occurring. Tracers such as temperature, potential temperature, and specific humidity can give insight on where different layers of the atmosphere are located and their properties when analyzing the vertical profiles and horizontal variation. For example, a strong inversion implies very little vertical mixing, suggesting that the particles originated in the marine boundary layer. The accumulation mode has been observed to dominate in the presence of a strong temperature inversion since the reduced vertical mixing allowed particles to grow into accumulation mode through condensation and coagulation with Aitken mode particles (Bates et al. 1998; Quinn et al. 2017). A marine surface air mass is characterized by an average relative humidity of approximately 80% (Royalty et al. 2017) with the relative humidity typically decreasing with height. This implies that lower relative humidity (e.g. 60%) could be indicative of subsiding air under a high-pressure system (Bates et al. 1998). A stable marine boundary layer results in longer residence times which can result in the growth of existing particles (Bates et al. 1998; Quinn et al. 2017). A residence time in the marine boundary layer of a few days or more (stable marine boundary layer) results in a significantly modified aerosol from the mixing of different aerosol sources. These distributions usually consist of a bimodal distribution with roughly equal contributions in number concentrations from the Aitken and accumulation modes

(Covert et al. 1996). The specific humidity can therefore be a useful tracer to determine an air parcel's origin. To summarize, there are limitations when using meteorology tracers to determine the origins of air parcels and their influence on the surface air, but assumptions can be made.

1.2.2 Marine Aerosols Sources and Their Unknowns

Marine aerosols are important because the oceans account for over 70% of the surface area on Earth. Along with being one of the largest primary sources of aerosols in the atmosphere the emission of sea spray aerosol is poorly constrained. Estimates of annual primary sea spray aerosol emissions generally range from 3 to 70 Pg yr^{-1} (Fitzgerald 1991; Grythe et al. 2014). This amounts to a very larger uncertainty in how much sea spray aerosol is emitted into the atmosphere. Studies in the field of atmospheric science have investigated sea spray aerosols in order to better constrain the number of aerosols emitted from the ocean, which will improve the uncertainty in the sources of aerosols in climate models. Overall, some sources of uncertainty in the marine boundary layer aerosol population include: the production, abundance, and mixing state of the aerosols; ocean emissions of trace gases such as VOCs; and long-range transport of continental aerosols. The number of aerosols and gases that enter into the marine boundary layer through entrainment is also a source of uncertainty. Quinn et. al, (2017) suggests that persistent, large scale meteorology features, such as high-pressure systems and fronts, entrain Aitken mode particles into the marine boundary layer which can affect the CCN activity.

Ambient aerosols in the marine environment can be classified as originating from marine or non-marine (continental) sources. The aerosols that make up the marine boundary layer can be

described as a mixture of primary sea spray aerosols (inorganic and organic), secondary non-sea-salt sulfate from the oxidation of ocean derived DMS, secondary ocean derived organics, marine VOCs (Ovadnevaite et al. 2014), and aerosol and gas precursors emitted from continental sources (Quinn et al. 2017). High levels of surface-active material can be found near shore and at high latitudes (Gantt and Meskhidze 2013). This surface-active material includes DMS oxidation products such as sulfur dioxide, sulfuric acid, dimethyl sulfide, dimethyl sulfone, and methanesulfonic acid can condense onto existing particles that can then grow. These compounds along with NaCl and methylsulfonic acid (MSA) can then be used as tracers for aerosols of marine source, whereas non-marine tracers include black carbon, radon, and hydrocarbon fragments (fossil fuels) (Sanchez et al. 2018).

The ambient marine size distributions often have multiple modes present due to emission of particles and atmospheric processes that grow particles by different mechanisms and at different rates (Seinfeld and Pandis 2016). These different modes can be used to determine the source of the particles observed in the marine boundary layer. The four main modes that are observed in the marine boundary layer are: a nucleation mode, Aitken mode, accumulation mode, and coarse mode, illustrated in figure 1.2. The nucleation mode is the smallest mode which consists of particles smaller than 20 nm and is composed of newly formed particles that can quickly grow through condensation into Aitken mode particles. However, the Aitken mode particles will most likely be lost due to diffusion and coagulation with the existing Aitken and accumulation mode particles (Bates et al. 1998). The Aitken mode consists of particles from 20 nm to 100 nm and most of these particles can grow into accumulation mode sized particles by vapour condensation of secondary material while transported in the atmosphere (Quinn et al. 2017). The accumulation

mode for marine particles consists of particles around 100 nm to 200 nm (Royalty et al. 2017) in diameter and is the result of primary emission, condensation of sulfates, nitrates, and organics, and coagulation with other particles. These accumulation mode particles are not readily lost in the atmosphere, which is the main reason why they accumulate. Lastly, the coarse mode consists of particles in the micrometer range in the size distribution which are composed primarily of sea salt in the marine environment and are generally produced by wind over the ocean (Bates et al. 1998).

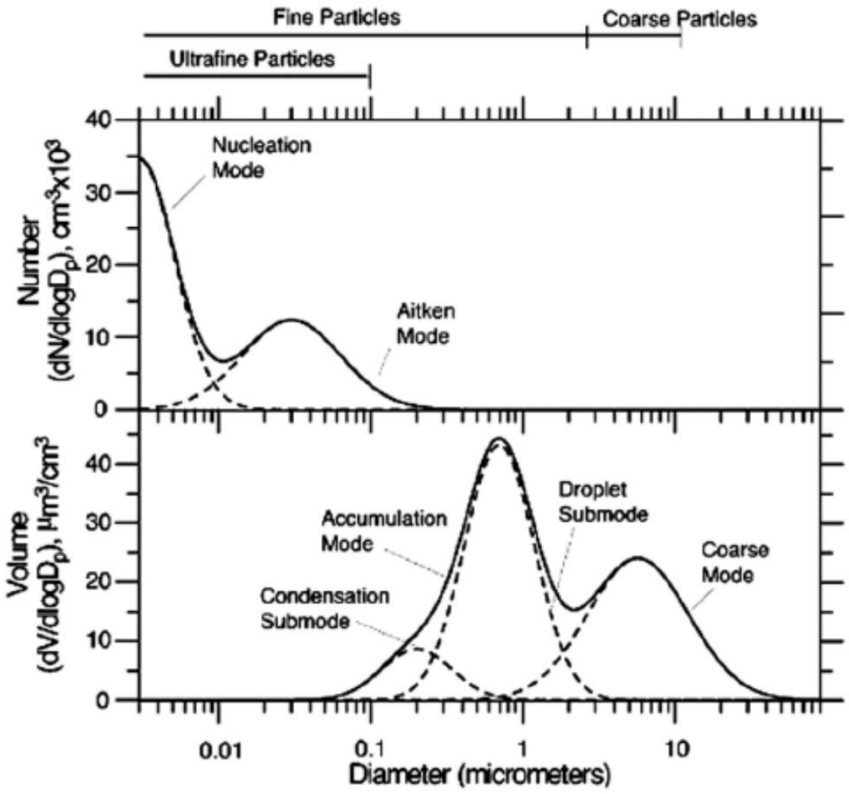

Figure 1.2: The different modes and submodes of the size distribution present in the atmosphere (Seinfeld & Pandis, 2016).

Sea spray aerosols include both sea salt and primary organic matter in the submicron sizes. Sea spray is injected into the atmosphere by the bubble bursting process which involves jet and film drops (Gantt and Meskhidze 2013) and shown in figure 1.3. Jet drops produce larger particles that originate from the bulk water (sea salt) whereas film drop produce smaller particles that are enriched in the surface microlayer which includes surface active organic material.

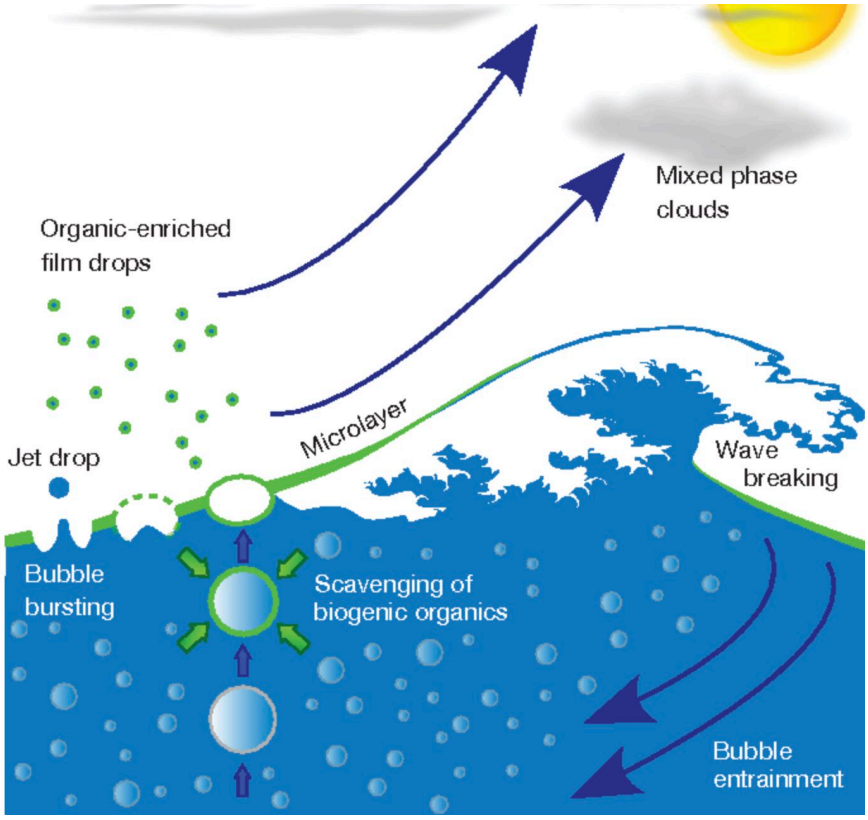

Figure 1.3: The production of sea spray aerosols by the bubble bursting process generated by breaking waves (Wilson et al. 2015).

Bubble bursting can be enhanced by high winds on the ocean surface (Gaston et al. 2011; Quinn et al. 2017). When high winds are present, sea spray particles dominate the marine CCN and particle concentrations (Bates et al. 1998; Zieliński 2004; Ovadnevaite et al. 2014; Sanchez et al.

2018), while DMS derived sulfate dominates at low winds speeds (Sanchez et al. 2018). There are conflicting reports of whether SSA contribute to accumulation mode particles when winds speeds are high (Bates et al. 2000; Quinn et al. 2017). This could be due to the fact that an increase in wind speed causes an increase in the flux of sea salt particles but can also increase the loss of SSA through sink processes (Bates et al. 2000). It has been shown that while particle concentration increases with wind speed, the size of particles that are being added are generally large (Hoppel et al. 1985). It has also been shown that particle concentrations shift from being dominated by larger particles to smaller particles at lower wind speeds (Gantt and Meskhidze 2013). Large gaps still remain in the understanding of SSA, where overall it appears that SSA are more abundant with higher winds, therefore contributing to an increase of particles in the accumulation and coarse modes.

Secondary aerosols are formed in the atmosphere through the production of gaseous precursors such as sulfuric acid, nitric acid, ammonia, organics, and VOCs. Secondary aerosols are important because they can modify the hygroscopic properties through gas to particle transfer, affect cloud processing, and participate in the production of secondary marine aerosols through nucleation events (Matteo et al. 2010; Royalty et al. 2017).

Secondary aerosols are produced in the marine atmosphere through the nucleation and condensation of vapours such as sulfuric acid and methanesulfonic acid which are formed from the oxidation of DMS, NO_x, and organics (Covert et al. 1992). The production of small particles in the marine environment is critically dependent on sulfuric acid concentration and the pre-existing aerosol surface area (Bates et al. 1998) since there is competition of acquiring the

available sulfuric acid and condensable vapors (Covert et al. 1992). When there are a significant number of particles that have relatively large sizes the gases are more likely to condense into growing existing particles rather than forming new ones (Pirjola et al. 2000). High DMS and low sea salt are needed in order to simulate particle formation. However, both DMS and sea salt production are correlated to wind speed with the sea salt particles acting as a condensation sink for the DMS oxidation products. An atmospheric process that could favor high DMS and low sea salt levels is precipitation (Pirjola et al. 2000). If precipitation preferentially removes SSA through CCN activation and wet deposition, then the DMS oxidation products can condense and form new particles in the absence of the existing particles.

For typical marine conditions, binary nucleation of water and sulfuric acid cannot be simulated for any realistic condition regardless of adiabatic cooling, turbulent fluctuation, advection, or entrainment from the free troposphere (Pirjola et al. 2000). This is because the rate of nucleation is strongly dependent on temperature, relative humidity, and the partial pressure of sulfuric acid and there are a number of processes both inside and outside the marine boundary layer that change the temperature and relative humidity in the marine boundary layer. However, there have been nucleation events simulated and observed when two air parcels are mixed together that have different temperature and relative humidities (Covert et al. 1992; Pirjola et al. 2000).

Bursts of small particles smaller than 10 nm in diameter have been observed in the past in the marine boundary layer (Bates et al. 2000; Sanchez et al. 2018). However, there is little evidence that nucleation actually took place in the marine boundary layer ((Bates et al. 2000; Sanchez et

al. 2018). In contrast, substantial evidence points to nucleation occurring in the free troposphere in the presence of DMS lofted from the surface (Pirjola et al. 2000).

1.3 Aerosols and Climate

Aerosols impact the climate by influencing Earth's radiation balance which measures the net energy balance between the energy received, from solar radiation, and the energy emitted, from the Earth through longwave radiation (IPCC 2013). The intergovernmental panel on climate change has developed a figure, shown in figure 1.4, to show how the major components present in the atmosphere contribute to the Earth's radiative forcing. The major components in the atmosphere can be grouped into four: the greenhouse gases, short-lived gases, aerosols and their precursor gases, and other, which consists of surface albedo and solar input.

As seen in figure 1.4, the uncertainty in the aerosol-cloud group is one of the largest since the understanding and contribution of the aerosol indirect effect on the climate is relatively uncertain (Haywood and Boucher 2000; Lohmann and Feichter 2005). The variability of the aerosol indirect effect on the climate's radiative forcing explains why the uncertainty for the aerosol cloud interactions is so large in figure 1.4. While clouds and aerosols have generally been shown to cool the climate, it varies spatially and temporally. A better understanding of aerosols and atmospheric processes involving aerosols is needed to better constrain climate models.

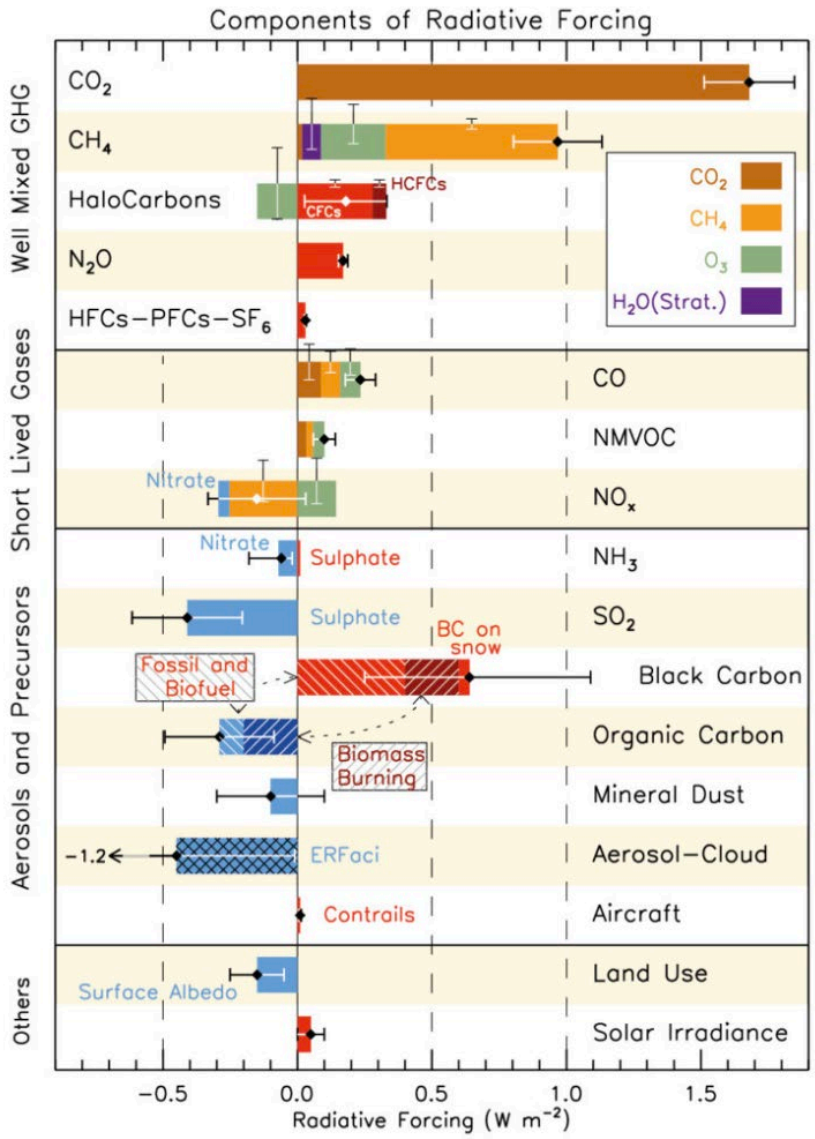

Figure 1.4: Radiative forcing of the major components in the atmosphere. The aerosol-cloud contribution shows the largest uncertainty in its radiative forcing on the climate (IPCC, 2013).

Aerosols in the atmosphere have multiple effects on the climate. The direct effect of aerosols is to scatter and absorb incoming solar radiation where the scattering contributes to the cooling of the climate by preventing solar radiation from reaching Earth's surface and the absorption warms local air masses, shown in figure 1.5. For example, sulfate particles scatter solar radiation

whereas black carbon particles absorb radiation which makes the direct effect variable and difficult to constrain when the physical properties of the aerosols are unknown. Aerosol physical properties such as the size distribution, number concentration, and composition determine the strength of the direct effect on the atmosphere (Charlson et al. 1992).

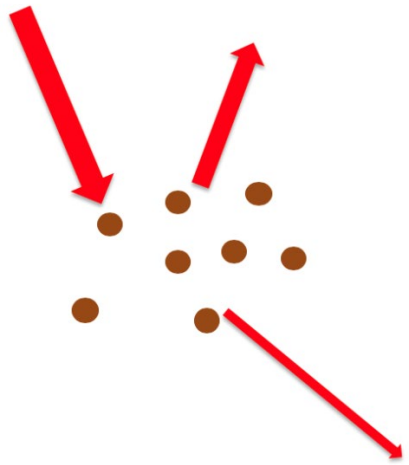

Figure 1.5: The aerosol direct effect accounts for scattering and absorption of incoming solar radiation.

Particles present in the atmosphere can act as cloud condensation nuclei (CCN) and grow into cloud droplets. The presence of these particles is necessary to form clouds because the smaller and therefore highly curved droplets have a large evaporation rate. This is because a curved surface has weaker bonds between the individual water molecules than a flat surface. This is known as the Kelvin effect. The curvature effect causes a need for a relative humidity greater than 100 %, a supersaturation of the atmosphere, for water vapour to transition from the gas phase to the liquid phase spontaneously. The presence of a CCN allows the droplet to start forming at a lower supersaturation to overcome the curvature effect of evaporation and provides a surface on which water vapour can condense without needing extremely high supersaturations.

When a particle grows large enough through the condensation of water vapour, it spontaneously becomes a CCN which then grows into a cloud droplet (Twomey 1991).

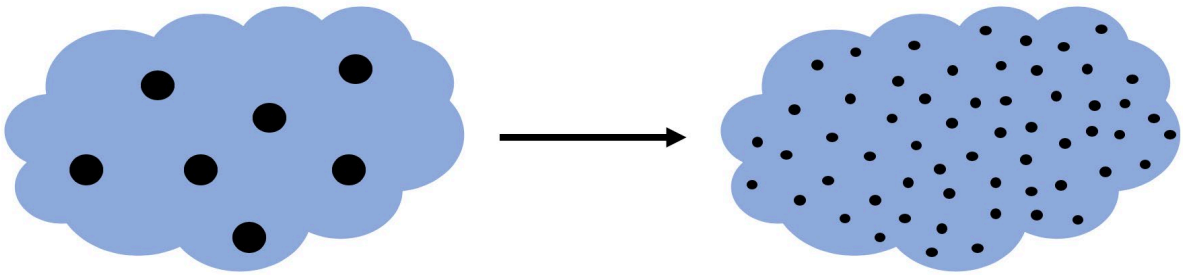

Figure 1.6: The indirect effect increases the reflectivity of clouds by increasing the number of cloud condensation nuclei but keeping the liquid water content of the cloud constant.

The aerosol indirect effect refers to the aerosols' effect on clouds through the concentration of aerosols present in the atmosphere (Wallace and Hobbs 2006) and is illustrated in figure 1.6. The aerosol indirect effect is also called the Cloud Albedo Effect (Twomey Effect) from Twomey and Warner, 1967, where they sampled cloud droplets and compared them to the cloud nuclei below the cloud base and found that these values positively correlated. The more aerosols present in the atmosphere, the higher the concentration of droplets present in the clouds. The concentration of cloud droplets present in a cloud is determined by the existing aerosol population. When the liquid water content of the cloud is constant, and more aerosols are introduced, the reflectivity, or albedo, of the cloud increases because more numerous smaller cloud droplets are present instead of a few larger droplets (Rosenfeld et al. 2019). This effect is important on the climate radiative forcing because clouds with higher droplet concentrations will reflect more radiation back to space, and therefore cool the climate. In the last century,

anthropogenic emissions of aerosols have increased and therefore the strength of the indirect effect has also increased. Twomey, 1977 shows that the recent addition of anthropogenic sources to the atmosphere influences the albedo of clouds. All clouds will scatter solar radiation back to space, with some aerosol absorption occurring if the clouds contain black or brown carbon.

1.4 Summary

In summary, there is a large amount of sea spray emitted into the marine boundary layer and it is poorly constrained. These emissions impact both the aerosol direct and indirect effect, which for the indirect effect, affect the amount of CCN available in the aerosol background. Understanding the background marine aerosols will improve our understanding of which aerosols have the potential to become CCNs under given atmospheric conditions. Part of understanding the background marine aerosols is characterizing the sources of these aerosols and the processes that modify these aerosols. This thesis characterizes aerosols so that their contributions to aerosol-cloud interactions can be better understood.

This thesis investigates the ambient marine particle size distributions during periods of processed marine air and harbour air. The understanding of the marine air and the processes involving these aerosols are important because these aerosols contribute to the indirect effect. The harbour air analysis is also important to understand how the aerosol emitted from industry in the harbours can contribute to the indirect affect and how they impact the population residing in these areas. In addition, two events are studied in more detail: an appearance of small particles and growth event, and a particle growth event. The origin of the air masses during these two events was

investigated to gain insight on the cause of these events and how they can impact the indirect effect.

Chapter 2: Methods

2.1 Sample Collection

This study was part of the Coastal Fog (C-FOG) study that investigated fog formation off the coast of Newfoundland. The sampling of ambient air was conducted on the R/V Hugh R. Sharp as it sailed from Lewes, Delaware on 31 August 2018, traveling near the coast of Eastern Canada, making stops in St. John's, Newfoundland on 11 September 2018, and Halifax, Nova Scotia on 18 September 2018, before returning to Lewes on 07 October 2018. Figure 2.1 shows a map of the ship's track, highlighting the special periods that will be discussed later

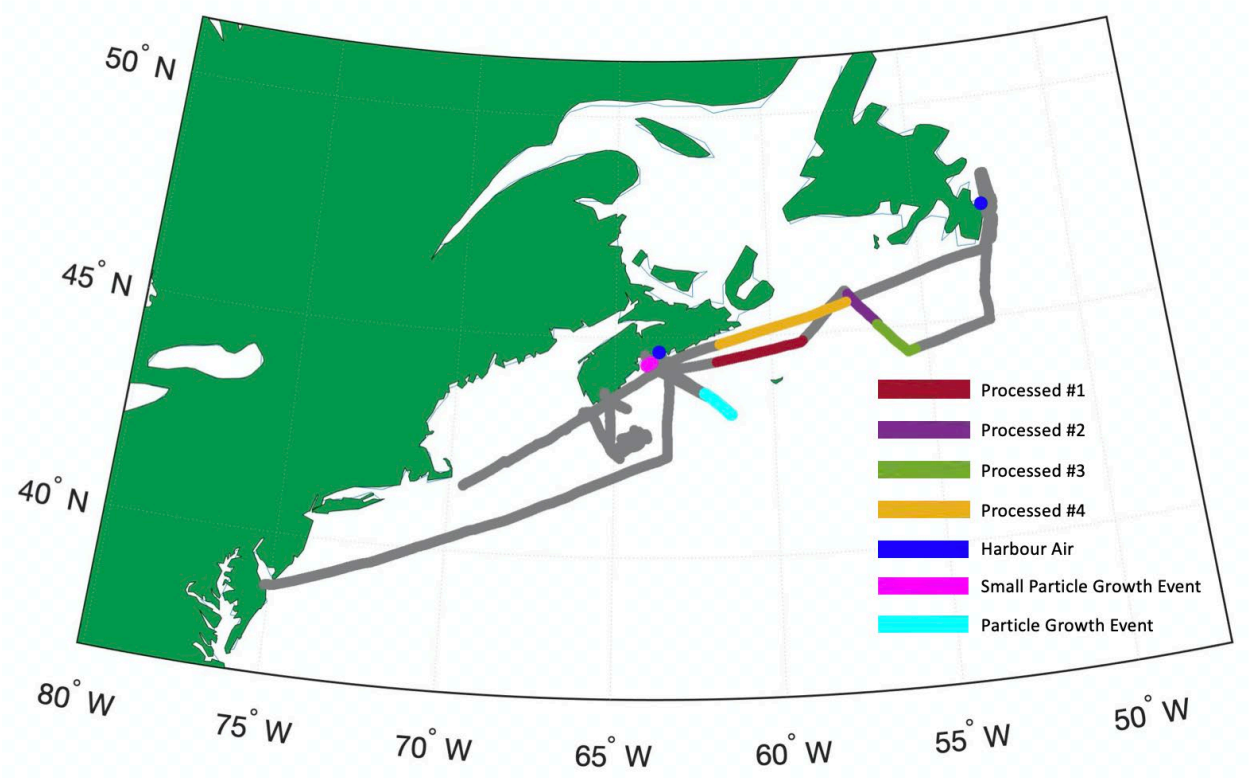

Figure 2.1: Ship track for the C-FOG Campaign. The grey line shows the entire route while the overlapping pink line shows the appearance and growth of small particles event, cyan line shows

the particle growth event, blue points show the harbour times, and the red, purple, green, and yellow lines show the processed marine air.

2.2 Inlet Description

The atmospheric aerosols were sampled through a custom-built inlet onboard the R/V Hugh R. Sharp with an intake 16 m from the bow and 12 m above sea level to minimize contamination from the ship. The inlet was designed to separate activated fog droplets from unactivated interstitial aerosols based on aerodynamic diameter, and therefore inertia, using a virtual impactor. Figure 2.2b shows a schematic of the inlet. The interstitial line in Figure 2.2b (left branch) only sampled aerosols smaller than 2.5 μm, which would correspond to interstitial aerosols in the presence of fog droplets. The droplet line (right branch in figure 2.2b) favored larger aerosols to pass through. The excess air in the interstitial line was vented after the virtual impactor so that it matched the flow rate of the droplet line. Once the aerosols were separated, they passed through silica dryers to evaporate water associated with these aerosols. The flow met a series of solenoid valves (Dynaquip) that switched every 30 minutes so that the instruments alternated sampling between the interstitial and droplet lines. The dried particles exited the inlet and were met with 0.9 liters per minutes of clean filtered air in order to make up the flow needed by the instruments. For this thesis, only the ambient data from the interstitial line was analyzed.

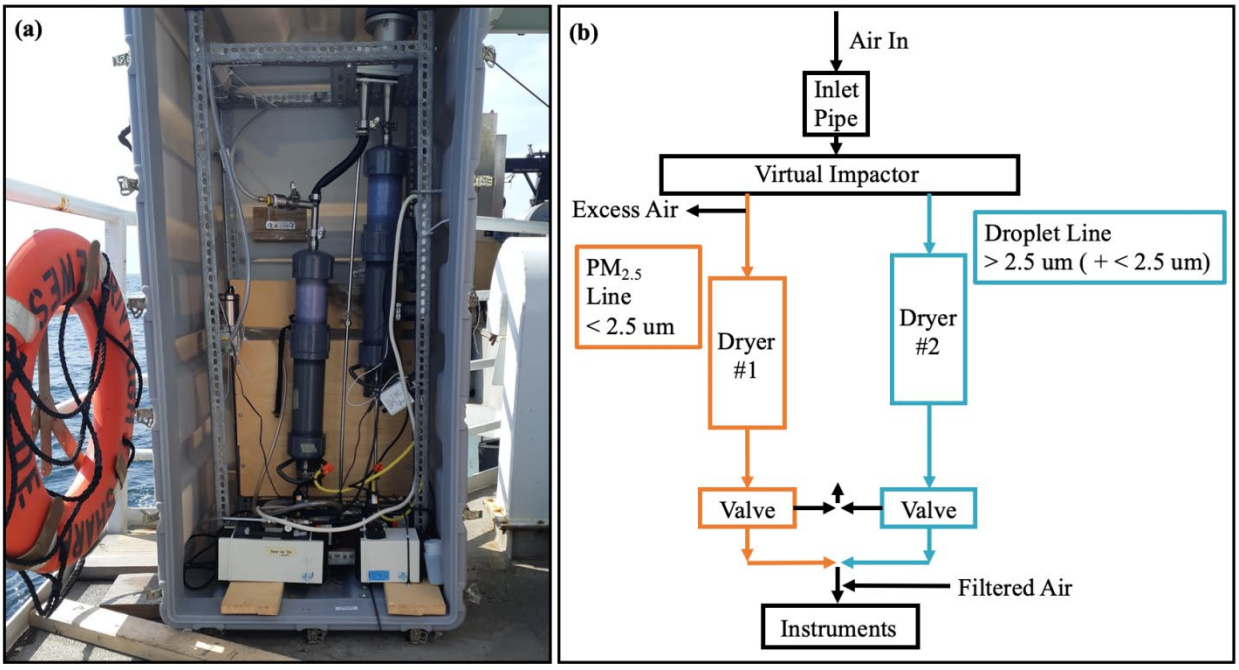

Figure 2.2: Photograph and schematic for the custom-designed inlet on board the R/V Hugh R. Sharp.

2.3 Instruments

Four instruments inside the ship measured aerosol size, composition, and CCN-activity (figure 2.3). These were the aerodynamic particle sizer (APS), the aerosol chemical speciation monitor (ACSM), the scanning mobility particle sizer (SMPS), and the cloud condensation nuclei counter (CCNC). For this thesis, only the size distributions were analyzed so instrument descriptions are limited to the SMPS and APS. Number concentrations were corrected by multiplying by a factor of 1.7 to account for the dilution flow added before the instruments.

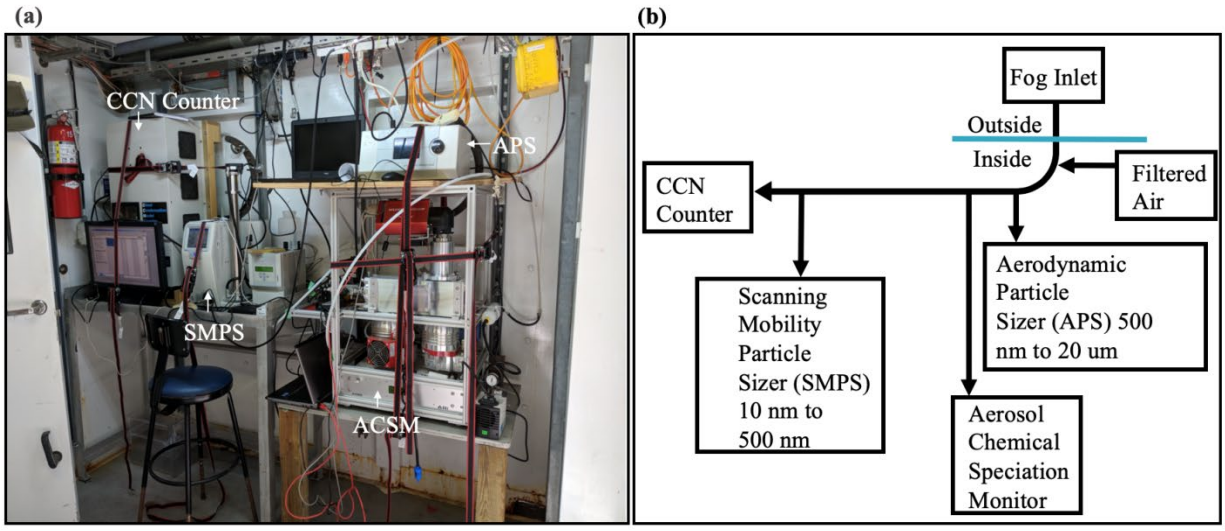

Figure 2.3: The four instruments on board the R/V Hugh R. Sharp used to measure aerosol size, composition, and CCN-activity.

2.3.1 Scanning Mobility Particle Sizer (SMPS)

Two instruments on board the ship measured the size distribution of the aerosols. The SMPS TSI detector model 3772 measured the smaller particles that ranged in size from 10.6 nm to 445 nm. For the C-FOG campaign, the SMPS was set up with a sheath flow of 5 l.p.m. and a sample flow of 1 l.p.m. with the sheath flow used to provide the flow of the particles through the differential mobility analyzer and the sample flow was the flow of the monodisperse particles. The SMPS was set up to measure scans on average every three minutes.

The SMPS is made up of an electrostatic classifier, differential mobility analyzer (DMA), and a condensation particle counter (CPC), where the electrostatic classifier and DMA together size select the particle and the CPC counts the particles at each given size.

At the inlet of the SMPS, a 0.072 cm impactor removed particles greater than 720 μm by forcing particles to turn 90°. Particles with too much inertia (i.e. larger diameter) were unable to complete the turn and landed on an impaction plate.

The polydisperse particle flow needed to be changed to a monodisperse flow in order to produce particle size distributions. The following explains the process of how a polydisperse flow changes into a monodisperse flow. The particles encountered a soft x-ray source in the electrostatic classifier that neutralized the particles and created a known particle charge distribution. The particles then flowed through the DMA which is composed of two concentric metal cylinders. The inside cylinder has a negative voltage and the outside cylinder is grounded thus creating an electric field inside the DMA through which the particles pass. Particles are size-selected based on their electrical mobility, their ability to move through an electric field (Knutson, 1975). For a given voltage on the inner rod, only a certain size of particle with a given charge can pass through the slit at the bottom of the DMA. Particles with a greater electric mobility get stuck to the inner rod and particles with a lower electric mobility miss the slit. The specific voltage therefore only allows a certain size to pass through the DMA giving monodisperse flow.

After the monodisperse particles exit the DMA they are counted by the CPC. Since it is difficult to use optical methods to count particles at sizes < 100 nm, the CPC grows the particles by first subjecting them to a heated chamber with vapourized butanol then passing the particles to a cooling chamber where the saturated butanol condenses onto the particles until they are large

enough to scatter light. The particles are then counted by converting the scattered light into electrical pulses which are then counted by a photodetector.

2.3.2 Aerodynamic Particle Sizer (APS)

The dried particles were also sampled by the APS model 3321 (TSI Inc.), which measured the particles from 457 nm to 13.4 μm and set up to scan on average every three minutes. The APS measures the aerodynamic diameter of the particles, which is obtained by measuring the velocity of the particles in the air flow based on their time of flight. A laser split into two laser beams points horizontally at photodetectors. When a particle passes through the first laser beam it scatters light from the laser and the break in the laser beam is detected by a photodetector. The break in the laser light is converted into an electric pulse. This is repeated in the second laser beam and the time between the pulses from the two lasers is measured. In the APS, the smaller particles accelerate faster than the larger particles through the air flow because of the inertia and lag on the larger particles. This indirectly sorts the particles by ordering them from smallest to largest. Knowing both the velocity of the flow and the time of flight, the aerodynamic diameter can be calculated (Seinfield and Pandis, 2016). The aerodynamic diameter is defined as the diameter of a unit density sphere of 1 g/cm^3 that has the same terminal velocity as the particle in question and can be converted into the actual particle diameter if the shape and density of the sampled particle is known. An assumed density of sea salt (2.16 g cm^{-3}) was used.

The APS has 52 size bins that range in size from 445 nm to 13 μm. The particles are binned immediately starting at the smallest size and going to the largest due to the fact that the smaller

particles accelerate faster and therefore pass through the laser first. After three minutes of measuring the aerosol sample, a size distribution is saved.

2.4 Data Analysis

2.4.1 Matching SMPS and APS Distributions

The data from the SMPS and APS were collected using the Aerosol Instrument Manager (AIM) software that stored the data files from the SMPS and APS. These files were then extracted into text files and analyzed using custom scripts in Matlab. The first step was to match the sampling time from the two instruments by creating a time wave that was continuous from the start of the sampling on 22:30:00 4 September 2018 UTC and increasing by three minutes until the end of the sampling on 04:27:00 6 October 2018 UTC. For simplicity, both the SMPS and APS scans were matched to the time wave instead of the time recorded for the scan. Since the SMPS and APS were set up to scan every three minutes the actual time of the scan was matched to the closest time on the time wave, within one minute and thirty seconds of the recorded end of scan time of the SMPS and APS.

As mentioned previously, the inlet switched between the interstitial line and the droplet line approximately every thirty minutes. However, the timing between switches varied slightly so uniform time intervals could not be assumed. To overcome this, the size distributions from the APS were used to determine which line was sampling. Since the interstitial line only sampled aerosols smaller than 2.5 μm, only sample times when the particle concentration in the 2.5 um bin was very low (< 10 cm^{-3}) were assigned as interstitial line distributions. APS scans were

matched with the time for the SMPS scans. The SMPS and APS scans from the interstitial line were combined to create one size distribution. There was overlap between the SMPS and APS sizes and therefore the number concentrations at those sizes in the distribution overlap. A continuous distribution was obtained by limiting the SMPS bins to below 445.1 nm and starting the APS bins at 456.8 nm.

2.4.2 Ship Emissions

The sampled air was inevitably exposed to ship's exhaust and therefore it was necessary to remove the data scans that were contaminated by ship emissions. The first step in removing the contaminated scans was to make a cumulative frequency distribution of the number concentration from the APS and SMPS combined. Only scans when the concentration was under 10000 cm^{-3} were kept in the data set, which included 95% of the data. This limit was used to cut off when the inlet was potentially sampling ship emissions. The very high concentration scans are most likely from the ship emissions and are not seen very often in the data set. This assumption only cuts out 5% of the data in order to keep as much ambient data as possible.

The next step was to eliminate ship emission using wind speed and direction. By looking at the placement of the ship's exhaust and the fog inlet, scans were eliminated when the wind direction was coming from the direction of the exhaust. Figure 2.4 shows the placement of the inlet in relation to the ship exhaust.

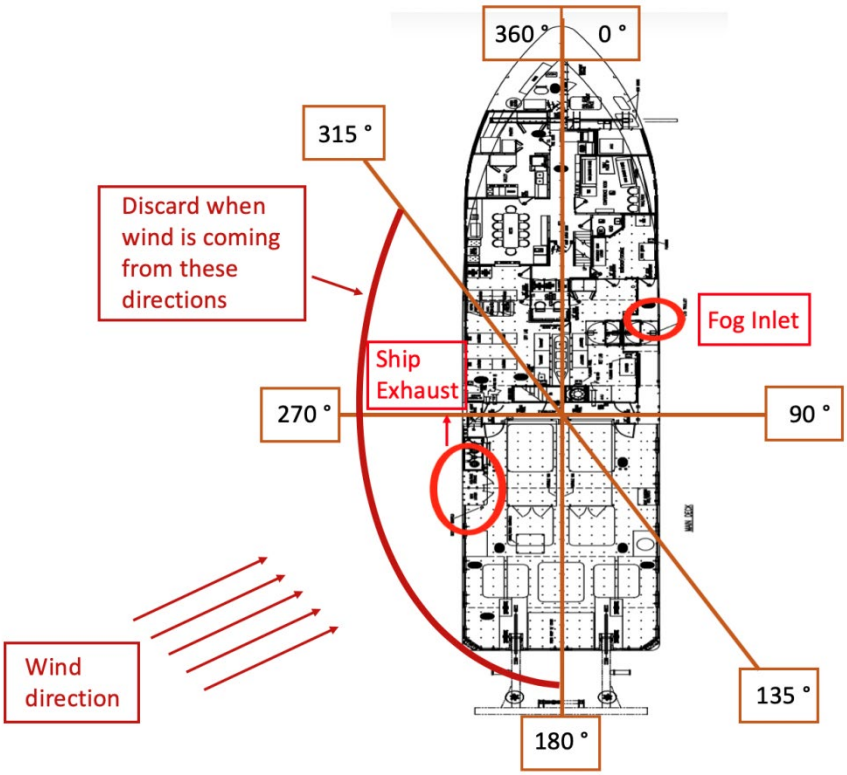

Figure 2.4: A schematic of the locations of the inlet and ship exhaust. Data associated with winds from 180 – 315 were excluded from the analysis.

The first step was to exclude wind speeds that were under 1 m s^{-1}. This ensured that the air was always moving and that no contamination from slow air mixing around the inlet was included. The next step was to filter by wind direction to exclude scans when the wind came from the directions near the ship's exhaust (less than 315° and greater than 180°). To try and keep the most data possible, a final filter was implemented so that when the wind was coming from the direction of the ship's exhaust, if the ship's speed was greater than the wind speed, then the scan was included because the inlet would have sampled particles coming from the front of the ship and not from the direction of the exhaust.

Filtering by wind direction was only used on the figures that use the whole data set and proved to remove too much data when looking at specific events that only lasted a few hours at most. To present a fuller picture during these events, the wind direction filter was ignored for the events analyzed in Chapter 3 because of their relatively short duration. The number concentration and size distributions were individually analyzed to determine if they were influenced by ship emissions, for example, when the concentration spiked for one scan and not the others as well as when the size distribution did not match the scan immediately before or after.

2.4.3 Auxiliary Measurements

There were multiple instruments on board the ship measuring temperature, wind speed, wind direction, and visibility. Temperature, relative humidity (HMP155, Vaisala) and wind speed and direction (IRGASON, Campbell Scientific) were measured on the bowmast of the ship at 12.5 m a.s.l. Radiosondes were launched from the aft deck to obtain vertical profiles of temperature and relative humidity in the atmosphere (iMet-3050A, InterMet Systems, Inc.). In total, 60 balloons were released throughout the whole cruise, generally around 0 UTC and 12 UTC with additional balloons released during events such as fog. The cloud coverage was determined with a Sky Camera and additional details of these systems are described by (Fernando et al. 2020).

2.5 MOUDI

The size-resolved aerosol chemical composition of soluble ionic components was measured by a Microorifice Uniform Deposit Impactor (MOUDI) (100NR, TSI Inc.) mounted above the pilothouse (12 m a.s.l.). The system consisted of 9 stages, with the nominal lower cut point of each

stage at 0.18, 0.32, 0.56, 1.0, 1.8, 3.2, 5.6, 10, and 18 μm. The MOUDI was only on board for part of the cruise, sampling from 13 September 2018 to 24 September 2018 UTC. The samples were analyzed using ion chromatography coupled with a conductivity detector to determine the mass loadings of Cl^-, NO_2^-, Br^-, NO_3^-, SO_4^{2-}, PO_4^{3-}, Li^+, Na^+, NH_4^+, K^+. Specific details, and the performance capabilities, of the anion and cation analytical methods are described by (Butz et al. 2017; Place et al. 2018). The separation of cations was performed with minor differences from Place et al. (2018) by using a CS19-4 μm (4x250 mm) analytical column operated at 35 °C with a dynamically regenerated suppressor (CDRS 600, 4mm, 3.9 V). The eluent gradient program was changed slightly by decreasing the maximum eluent concentration from 10 mM MSA to 8 mM resulting in a total run time of 44 minutes.

2.6 HYSPLIT Trajectory Model

NOAA Air Resources Laboratory developed a Hybrid Single-Particle Lagrangian Integrated Trajectory (HYSPLIT) model for calculating air parcel trajectories with its most common use of back trajectory analysis to determine air mass origins. The HYSPLIT back trajectory model uses a hybrid between the Lagrangian method of following the air parcel and the Eulerian method of using a fixed space in order to provide the best estimate of an air parcel's origin (Stein et al. 2015).

The HYSPLIT allows multiple options for the archived weather models used to determine the back trajectory. For this thesis the model used for the weather domain was the North American Mesoscale (NAM) Forecast System [12 km] because it is the highest resolution model available

and therefore would provide the best output of the air parcels' backward trajectories. The NAM is one of the major regional weather forecast models and is run by the National Centers for Environmental Prediction (NCEP) and uses a 12 km horizontal resolution Lambert Conformal grid and runs every 6 hours (00, 06, 12, 18 UTC). For trajectories outside of the NAM domain, the Global Forecast System (GFS) at 0.25° resolution was used instead. The model was run in Normal mode using model vertical velocity as the vertical motion to calculate 48-hour back trajectories. The location of the starting points were the GPS coordinates of the ship at the start of each event.

Chapter 3: Results and Discussion

This thesis will focus on aerosol size distributions of processed marine aerosols, harbour emissions in Halifax, Nova Scotia and St. John's Newfoundland, and two case studies: an small particle appearance and growth event as well as a particle growth only event. The goal of the two case studies was to determine the origin of the air parcel and the conditions leading up to each event. Determining the sources and processes of aerosols in the marine boundary layer is important to improve our understanding of the contribution of aerosols to climate. The data in this thesis was sampled at the surface at the location of the ship at a certain time and from a single vertical column above the ship. The horizontal advection changes are assumed to be minor.

3.1 Processed Marine Air

The time series of the particle size distributions and total concentration for the whole cruise duration are shown in figure 3.1. The days used for determining the processed marine air were the transit from Halifax to St. John's, September 6 to September 8 and the transit back from St. John's to Halifax, September 16. The specific dates and time are listed in table 1.1 and shown in the green boxes in figure 3.1. The criteria for determining the processed marine air were: using only times when the ship was in transit so that the air was always in motion, using times when there was no precipitation and minimal clouds so that there were no influences from deposition from precipitation, and the ship had to be at least 50 km from any coast to minimize continental influence. The samples were also filtered as described in section 2.4.2.

Table 1.1: The dates and times (UTC) for the cases discussed in this section.

Air Sample	Date and Time (UTC)
Processed Marine Air Sample #1	00:24 6 September 2018 – 17:39 6 September 2018
Processed Marine Air Sample #2	13:48 7 September 2018 – 23:48 7 September 2018
Processed Marine Air Sample #3	00:30 8 September 2018 – 16:06 8 September 2018
Processed Marine Air Sample #4	00:03 16 September 2018 – 9:42 16 September 2018
St. John's Harbour	11:00 11 September 2018 – 14:30 12 September 2018
Halifax Harbour	12:10 17 September 2018 – 11:00 19 September 2018
Small Particle Appearance and Growth Event	15:00 20 September 2018 – 19:00 20 September 2018
Particle Growth Event	16:00 23 September 2018 – 00:00 24 September 2018

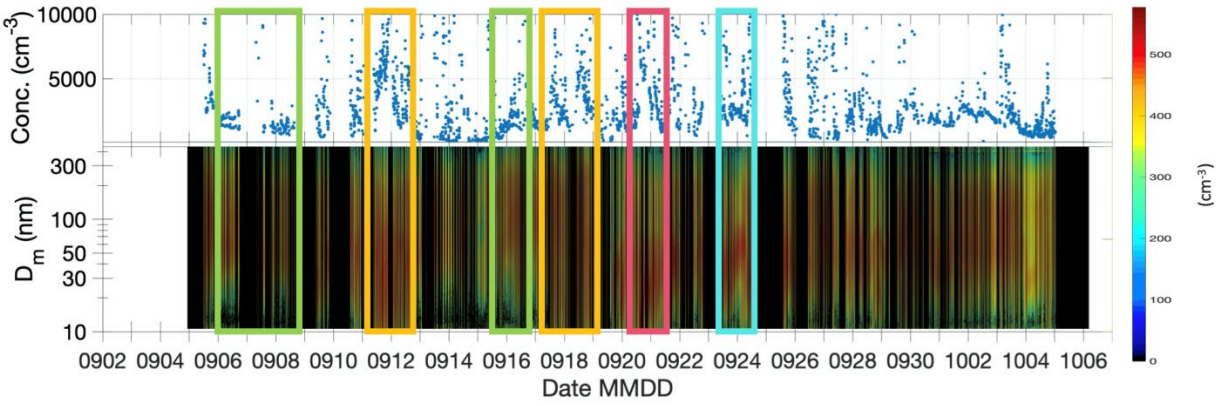

Figure 3.1: Time series of total particle number concentration on top and particle size distributions on the bottom. The green box indicates processed marine air, yellow box indicates harbour air, pink box shows the small particle appearance and growth event, and blue shows the particle growth only event.

For the processed marine aerosol, the average particle concentration over all of the samples selected was 1394±437 cm^{-3}, where the uncertainty is the standard deviation, and their average size distributions are shown in figure 3.3. During the cruise, two types of background marine distributions were observed which consisted of bimodal distributions that had been cloud processed and single mode distributions from aged aerosols.

Focusing on the time period from 6 to 8 September, processed marine air samples #1, #2, #3, these average size distributions show clear Aitken and accumulation modes at around 50 nm and between 100 nm and 150 nm, respectively. The average total number concentration for the processed marine air for these three samples selected was 1363±190 cm^{-3}. These bimodal distributions are consistent with aerosols that have been cloud processed (Hoppel et al. 1985), where some Aitken mode particles activate into cloud droplets, grow through in-cloud processes

and turn into accumulation mode particles when the droplets evaporate. The Hoppel minimum represents the minimum between the peaks in bimodal size distributions and is theorized to be the size of the minimum activation diameter of the cloud. Assuming the particles were composed of ammonium sulfate ($\kappa = 0.6$) and using the Hoppel minimum as the activation diameter (80 nm – 100 nm) the supersaturation of the clouds is estimated to be between 0.16% and 0.21%. Bimodal distributions are not always caused by cloud processing, other possibilities include: the mixing of two different air masses, growth of larger particles through direct condensation, and the production of particles at the smaller sizes (Hudson et al. 2015). The HYSPLIT back trajectories, shown in figure 3.2, showed that the bimodal distributions all have marine influence and came from above the surface layer. This further suggests that these aerosols were cloud processed, creating bimodal distributions.

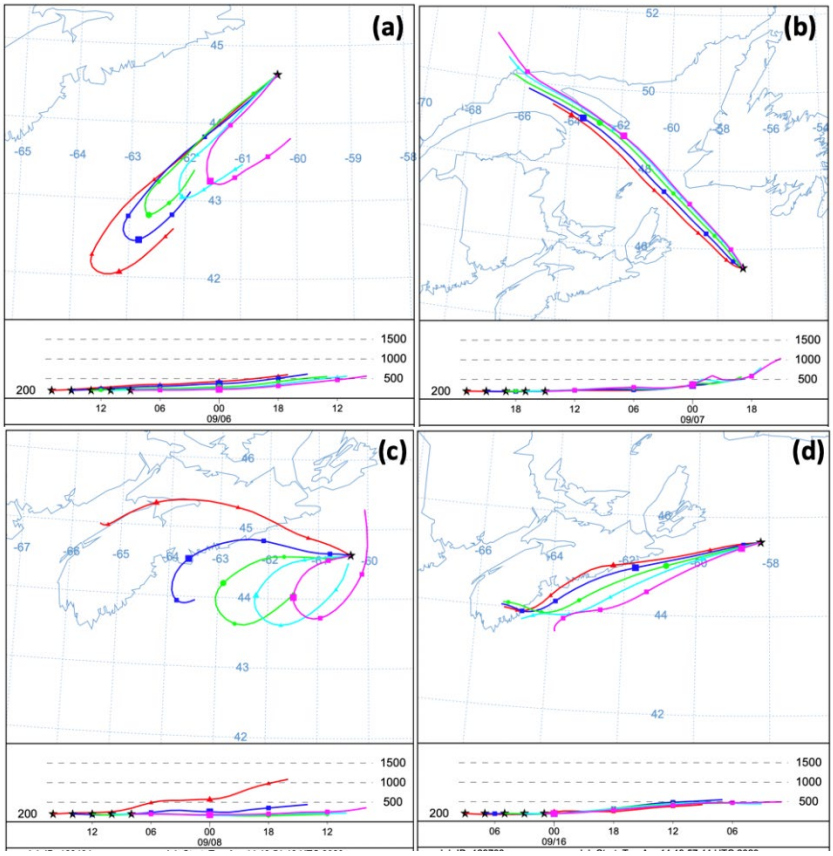

Figure 3.2: The NOAA HYSPLIT backward trajectories for: (a) 6 September, (b) 7 September, (c) 8 September, and (d) 16 September.

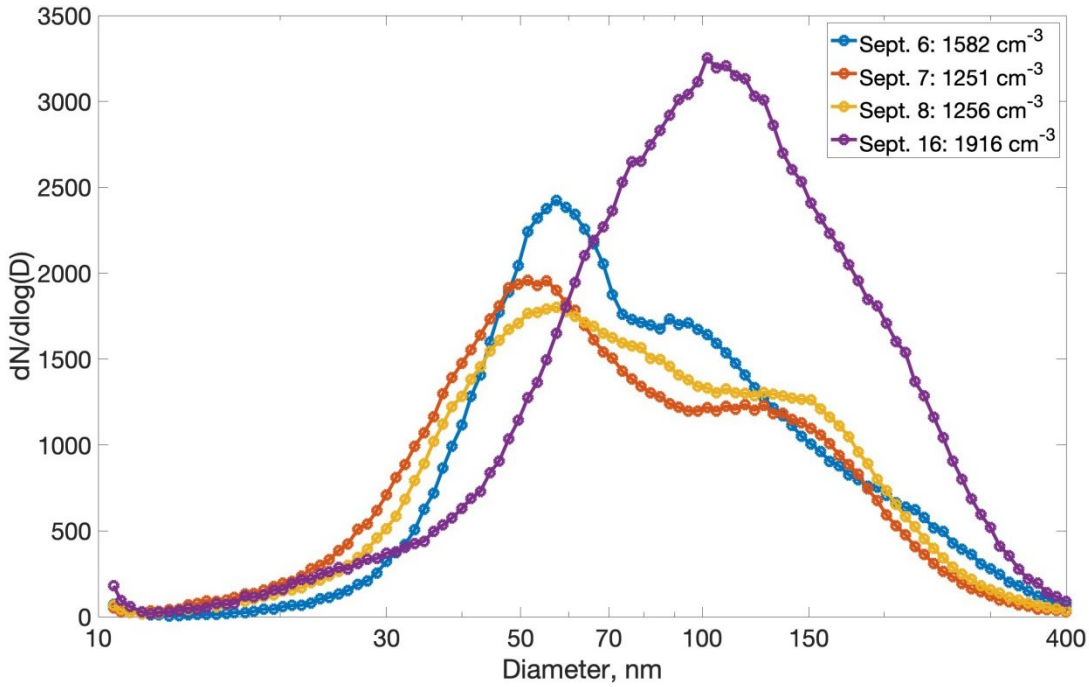

Figure 3.3: Average size distributions and their average total number concentrations for the four processed marine air samples listed in Table 1.1.

The 16 September distribution appears to be from different sources when compared to the other background samples. The 16 September sample showed a single broad peak at around 150 nm with no Aitken mode present, unlike the samples from 6 to 8 September. A potential reason for the difference between the distributions selected could be due to passing weather patterns. In the case of 16 September, the absence of the Aitken mode implies that the aerosols were aged, meaning that any prior Aitken mode particles had either grown into the accumulation mode due to condensation of precursor gases, coagulated with the larger existing aerosols in the accumulation mode, or wet scavenged by precipitation. The weather during this period started on 14 September with a cold front to the north which transitioned into a stationary front by the end of the day on 14 September with overcast skies persisting until the end of the day on 15 September when the stationary front dissipated. A high-pressure system moved over the location

of ship late on 15 September, providing clear skies on 16 September until the end of the sample, approximately 9:30 UTC. The front on 14 September caused precipitation and essentially cleaned out the existing background aerosol population through wet scavenging and wet deposition. The high-pressure system approached the ship's location from the southeast, bringing air that had been over the northeastern United States for three days. Due to the fact that the ridge was slow moving, the aerosols in that air mass had the opportunity to age. This could explain the presence of only a large accumulation mode in the particle size distribution in figure 3.3. The HYSPLIT back trajectory, shown in figure 3.2, for the 16 September sample showed air moving along the coast and over the province of Nova Scotia with the air parcel in the boundary layer at least 24 hours before.

Of all the processed marine aerosol cases, the MOUDI only sampled during the 16 September case. Figure 3.4 shows the size-resolved chemical composition of the water-soluble inorganic components. As expected, the sodium and chloride components were found in the marine air in the coarse mode. There was also nitrate present in the coarse mode, which could be from continental influence such as coal combustion, natural gas burning, and vehicle emissions (Zhang et al. 2014). Nitrate in the coarse mode suggests chloride displacement from sodium chloride by nitric acid. This would be consistent with a continental air parcel mixing with a marine air parcel containing sodium chloride, further providing evidence of aged aerosol. The nitrate displacement with chloride in the coarse mode indicates that the air parcel had the opportunity to ages, most likely in the MBL.

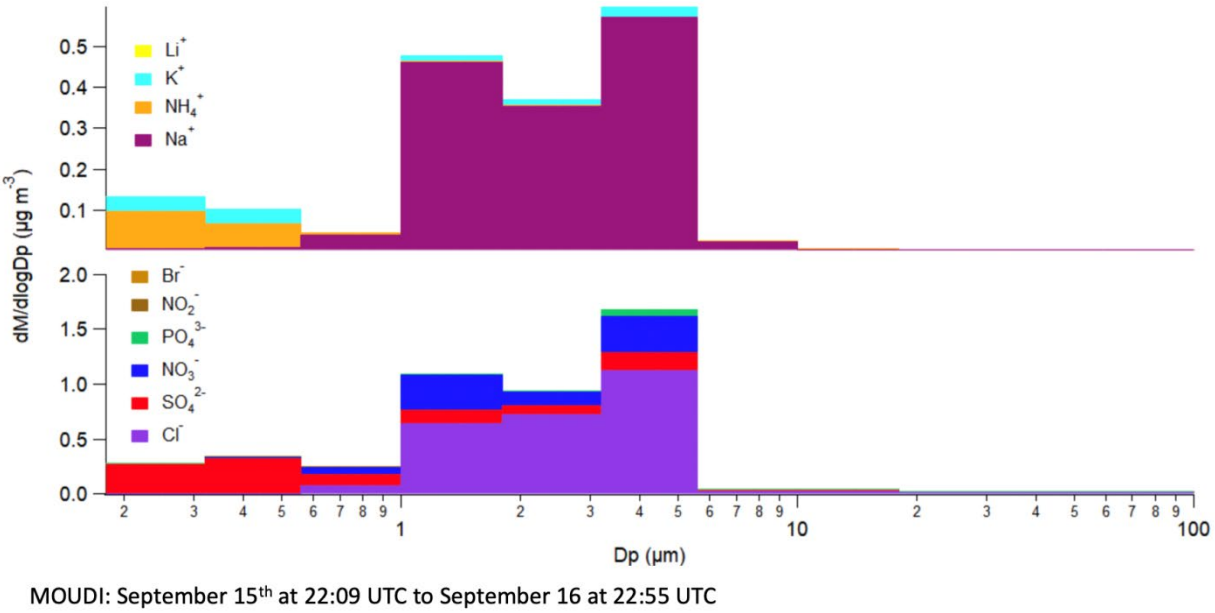

Figure 3.4: MOUDI mass concentrations during the 16 September processed marine air event.

3.2 Harbour Air

The average particle size distributions when the ship was in the St. John's and Halifax harbours are shown in Figure 3.5 along with their average total particle number concentration. The size distribution in the St. John's harbour, shown in blue, was larger and had more Aitken mode particles compared to the size distributions in the Halifax harbour (orange, yellow, and purple lines), where a broader peak spanned the Aitken and accumulation modes. A higher average total number concentration of 6338±4326 cm^{-3} was observed in the St. John's harbour which is almost double the average total number concentration of the Halifax harbour at 3339±3075 cm^{-3}. Also shown in figure 3.5 are the processed marine air size distributions (grey) as a comparison to the size distributions in the harbours. As expected, the processed marine air size distributions have smaller number concentrations at all sizes with the highest concentrations between 50 nm and

200 nm. In contrast, the harbour distributions show more particles at the smaller sizes, especially the St. John's size distribution.

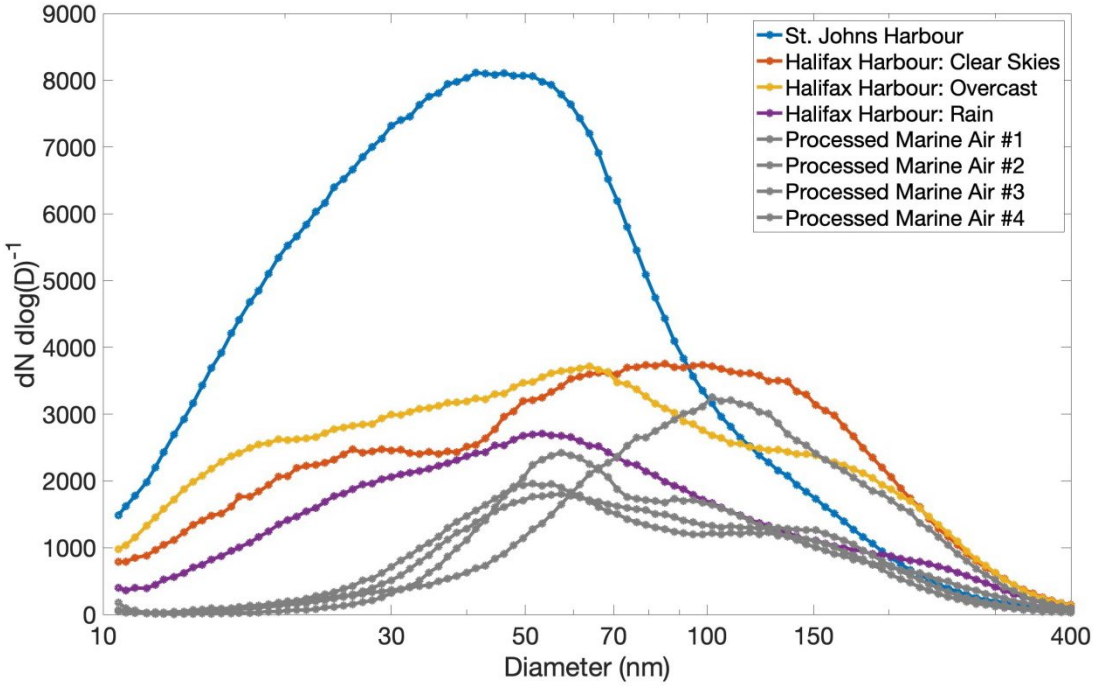

Figure 3.5: The averaged particle size distributions for the St. John's and Halifax harbours along with their average total particle number concentrations. The grey lines show the processed marine air for comparison.

The shift to the smaller but more numerous particles in the St. John's harbour suggests greater harbour emissions and pollutants compared to the Halifax harbour. A possible reason for this is that the St. John's harbour is more contained and geographically restricted by hills surrounding the harbour and downtown area. This causes emissions from the harbour and downtown area to build up due to less ventilation. On the other hand, the Halifax harbour is more spread out with a

significant amount of open space and little topography, allowing greater ventilation of any harbour emissions.

Another possible reason for the difference between the harbour air in St. John's and Halifax could be the present weather that occurred during these times may have modified the aerosol population. The weather when the ship was in St. John's started with a high-pressure system over mainland Newfoundland and continued over the harbour until a low-pressure system approached from the south just before the ship left the harbour. The high-pressure system lasted for the majority of the time the ship was in the harbour and contributed to a light average wind speed of 3.6 ± 1.5 m s^{-1}. The topography and light surface winds in St. John's would be favourable for the aerosol concentration to build. The smaller aerosols observed are consistent with emissions from local sources such as the harbour and down town.

While sampling in the Halifax harbour, the SkyCam equipped on the ship showed overcast conditions that transitioned into clear skies after 4 hours. The clear skies lasted for 5 hours and then transitioned back into overcast with rainfall until the ship exited the harbour. The size distributions corresponding to the different weather conditions are shown in figure 3.5. Archived surface analysis showed a high-pressure system to the south with a trough of low pressure moving towards Halifax accompanied with an average wind of 2.5 ± 1.5 m s^{-1}. The clear skies when the ship initially entered the harbour corresponded to a size distribution dominated by the accumulation mode (orange line in figure 3.5) with a small Aitken mode present as well. The larger accumulation mode suggests aged particles and the Aitken mode suggests local emission of particles. There was also nitrate present in the coarse mode and all this suggests that there are

fresh aerosol emissions overlaid on an aged background aerosol. In contrast, the Aitken mode dominated during the rain (purple line in figure 3.5) because the larger particles were wet scavenged and not sampled by the interstitial line. The precipitation could explain the low concentration of particles compared to the St. John's harbour as well as the overcast and clear skies distributions in the Halifax harbour.

Figure 3.6 shows the size-resolved aerosol mass concentration measured by the MOUDI for the time the ship was located in the Halifax harbour. The ship was actually in the harbour from 12:00 17 September 2018 UTC to 10:30 19 September 2018 UTC, which spanned the two MOUDI samples shown in figure 3.6. Nitrate in the coarse mode and sulfate and ammonium at the submicron sizes are major components of the aerosol mass, likely due to industrial emissions in the harbour such as shipping container terminals, medium sized oil refineries, and cargo piers. Downtown Halifax is also close to the harbour and could have contributed emissions from food industry and automobiles. Coal combustion and natural gas burning are a major source of sulfate as well as nitrate with nitrate also being sourced from vehicles (Zhang et al. 2014). Off the coast of Nova Scotia there are also several natural gas production platforms that could have also contributed to the concentrations of nitrate and sulfate in the aerosols. Ammonia is also expected in a harbour setting because it can be emitted from industry in the anthropogenic sense but also has natural sources such as birds which are also present in most harbours (Air Pollution Information System, 2006), but there may not be enough birds to account for the ammonia concentrations observed. It is interesting to note is that while ammonium and sulfate concentrations were observed at multiple times throughout the cruise, the concentration of nitrate was the highest in the coarse mode during the time the ship was approaching and, in the Halifax

harbour. As discussed previously, high nitrate levels in the coarse mode is likely due to chloride displacement as NaCl ages through interactions with continental influences (Zhang et al. 2014). Unfortunately, no MOUDI measurements were available when the ship was in St. John's harbour.

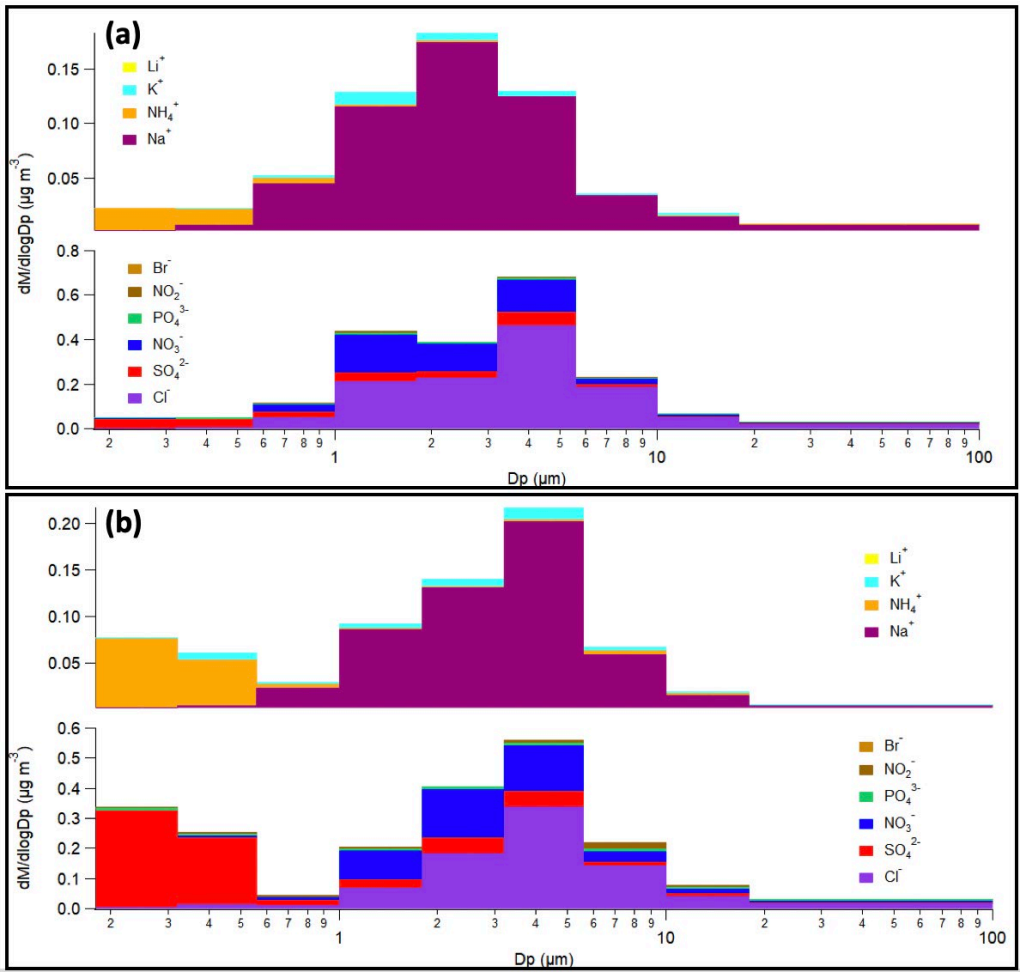

Figure 3.6: MOUDI aerosol mass concentration during the time the ship was located in the Halifax harbour. Panel (a) measured from 23:30 16 September 2018 UTC – 9:43 18 September 2018 UTC and panel (b) from 15:13 18 September 2018 UTC – 16:51 19 September 2018 UTC

3.3 Small Particle Appearance and Growth Event

From 15:00 20 September 2018 UTC to 19:00 20 September 2018 UTC a burst of small particles with a diameter of 10 nm suddenly appeared and grew to 30 nm over four hours, as shown in figure 3.7. During this time the weather observations were clear skies that turned into scattered clouds by the end of the day. At the start of the event the particle concentration rose by almost 2000 cm^{-3} and remained constant during the event. The increase in number concentration suggests that these small particles were added to the marine boundary layer.

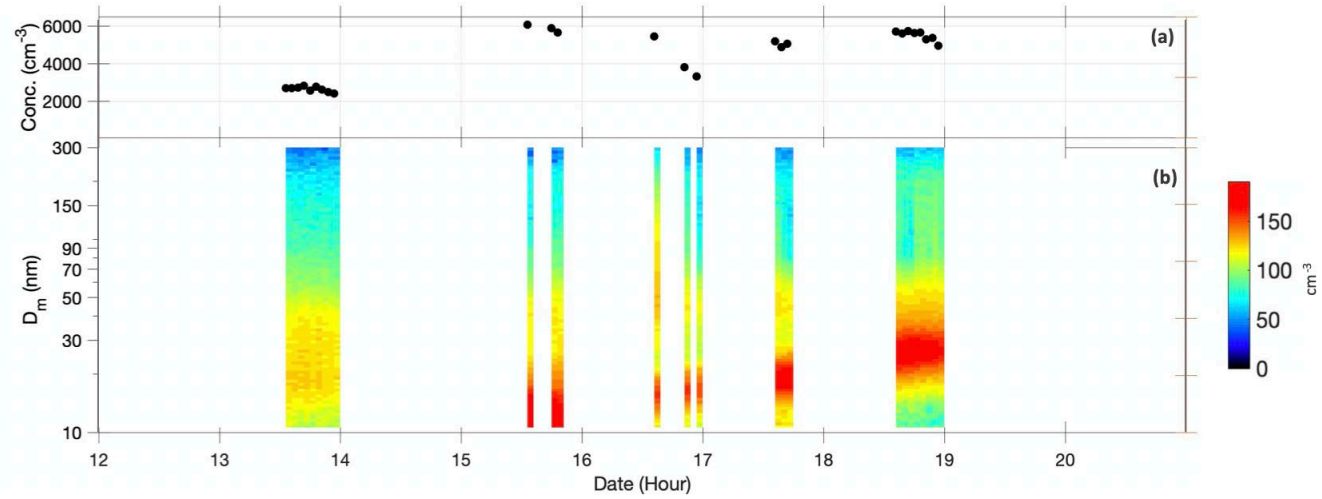

Figure 3.7: Shows the total number concentration, panel (a), and the particle size distribution over time, panel (b), for the small particle appearance and growth event.

It is difficult to determine whether the nucleated particles formed in the boundary layer or in the free troposphere before descending and growing. Covert et al. 1996 and Pirjola et al. 2000 suggest that nucleation in the marine environment is prominent in the free troposphere where the condensation sink is low and large amounts of the precursor gases are available. These

conditions arise because the temperature inversion at the top of the marine boundary layer prevents mixing into the free troposphere. However, it is possible that nucleation can occur in the marine boundary layer if the conditions are favourable especially in the fall and winter months (Sanchez et al. 2018). The following discusses the possible height at which nucleation took place, exploring the possibility that the nucleation took place in the free troposphere and subsided or nucleation occurred in the boundary layer and mixed with the surface. Meteorology variables at the surface and throughout the column were investigated in addition to the aerosol chemical composition to gain insight on the sources of the air. Backward trajectories from the NOAA HYSPLIT model were also analyzed to determine the origin of the air parcel.

The first step was to examine the pressure, temperature, relative humidity, and specific humidity at the time of the event. Figure 3.8 shows these variables around the time of interest with the red boxes indicating the actual time of the event.

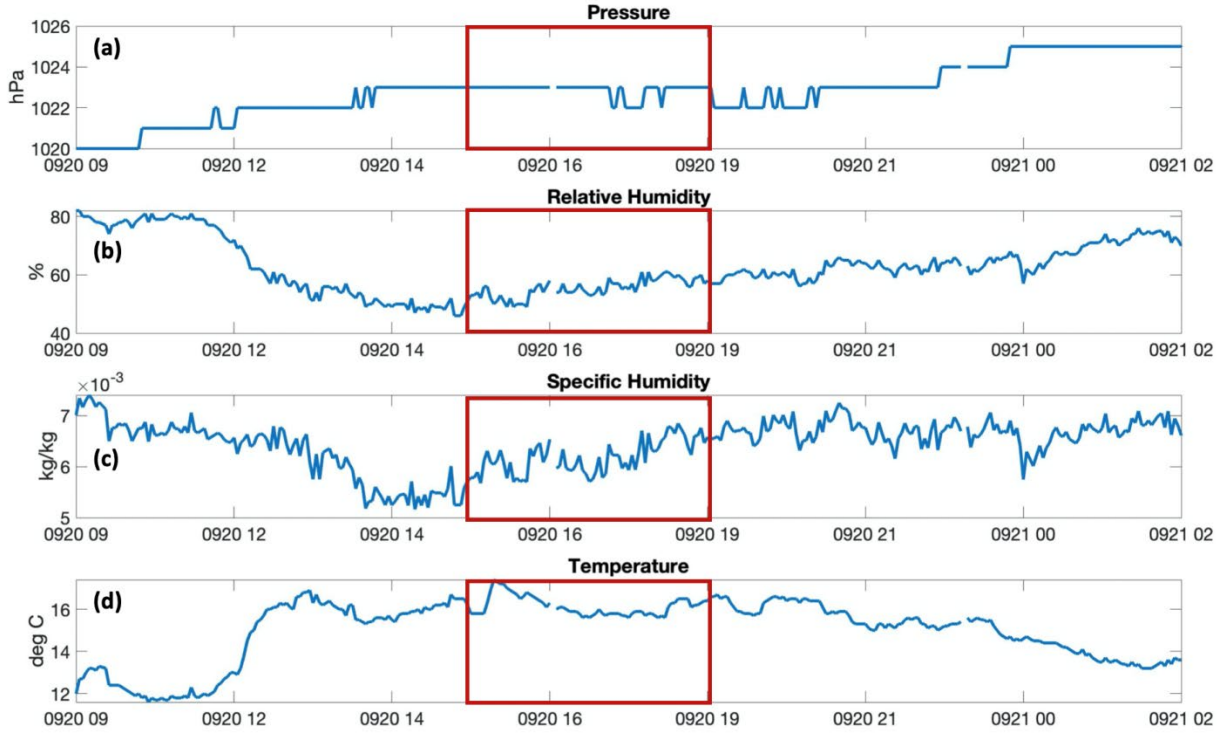

Figure 3.8: Pressure, relative humidity, specific humidity, and temperature are plotted during the and appearance and growth of small particles event. The red boxes indicate the actual time the small particles appeared and grew.

The first point to note is the rising pressure that was observed over the entire time shown in the plot which generally indicates subsiding air from above into the surface layer, although, the pressure was relatively constant during the actual event. The surface analysis corroborated the presence of a high-pressure system at the location of the ship. Figure 3.9 shows the surface analysis from the National Weather Service Weather Prediction Center archives. Figure 3.9a shows a low-pressure system to the south of Nova Scotia and the ship (green dot) as well as a high-pressure ridge over Quebec and the eastern United States. During the event (figure 3.9b), the high-pressure ridge moved towards the location of the ship, and finally after the event, a

ridge of high pressure remained over the location of the ship and the Maritimes (figure 3.9c). Overall, this could indicate large-scale subsidence associated with the high-pressure system.

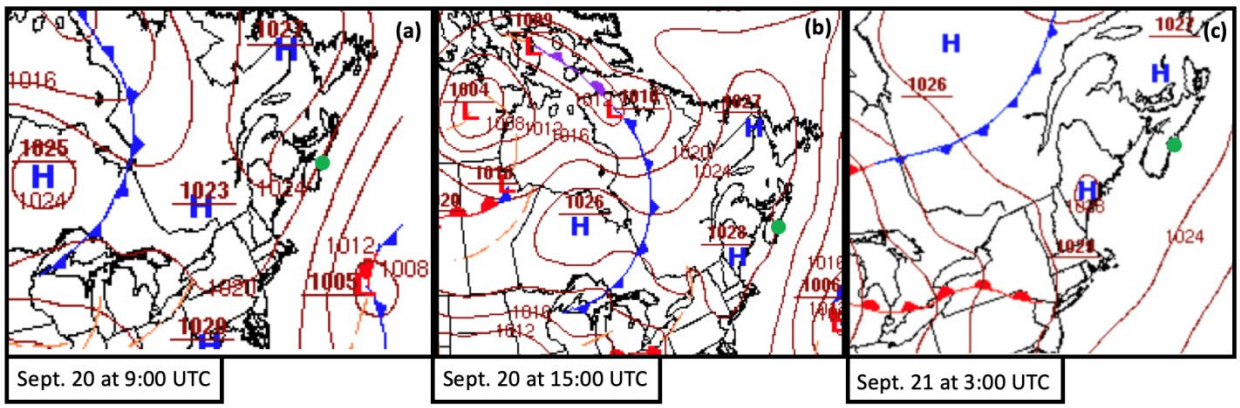

Figure 3.9: The surface analysis plots for the appearance and growth of small particles event showing (a) the start of the event, (b) during, and (c) after the event (NOAA, 2015). The green dot indicates the location of the ship.

The specific humidity at the surface also changed significantly before the event started, suggesting that different air had mixed into the surface layer at 12:00 UTC. The specific humidity decreased before the small burst of particles was observed (figure 3.8c), consistent with dryer air mixing with the moister surface layer, which decreased the water content of the surface parcel.

Studies from the North Atlantic and North Pacific Ocean by Sanchez et al. 2018 and Covert et al. 1996, respectively, observed the presence of nucleation mode particles that subsided into the marine boundary layer from the free troposphere. Covert et al. 1996 concluded that little particle production was observed in the marine boundary layer and that most of the nucleation mode and

Aitken mode particles originated in the free troposphere before subsiding into the marine boundary layer through large scale subsidence or post-frontal subsidence. Sanchez et al. 2018 also investigated the origin of newly formed particles by looking at the strength of the boundary layer inversion that separates the marine boundary layer and the free troposphere. They found that newly formed particles negatively correlated with inversion strength, meaning that newly formed particles were found when the boundary layer inversion was weak. This latter study concluded that there was substantial evidence of particle nucleation occurring after DMS was lofted into the free troposphere.

To investigate if the origin of the air mass was the free troposphere, the vertical profile of the temperature, potential temperature, and specific humidity of the atmosphere were analyzed. Figure 3.10 shows these variables at 11:14 20 September 2018 UTC, and at 23:13 20 September 2018 UTC.

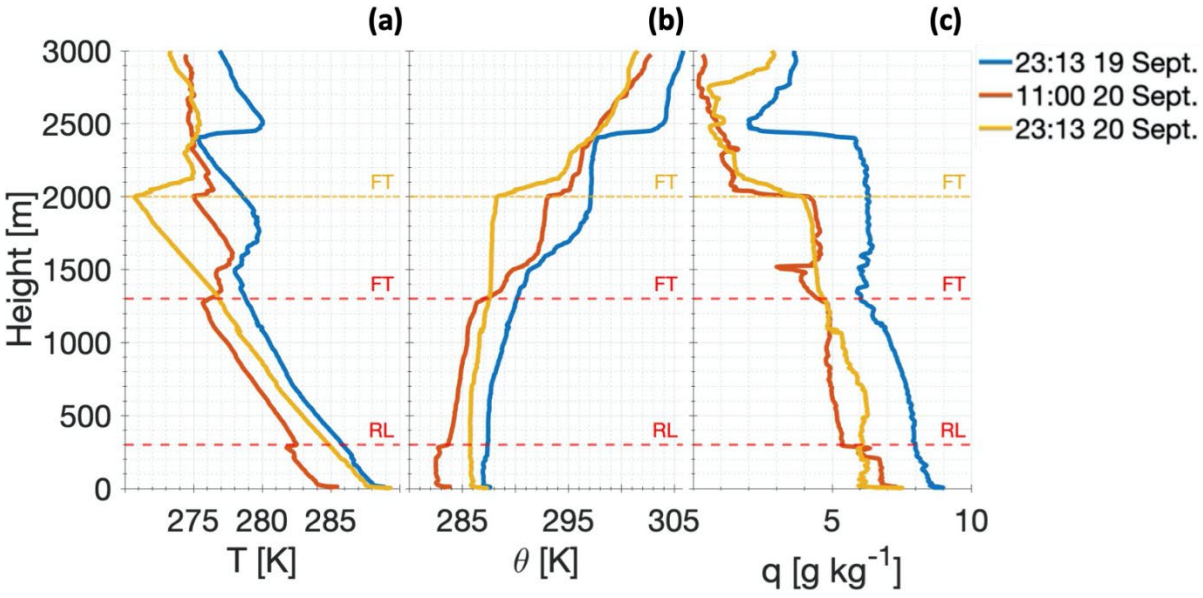

Figure 3.10: Vertical profiles of temperature, panel (a), potential temperature, panel (b), and specific humidity, panel (c), from the radiosondes. The blue lines are from the radiosonde at 23:13 19 September, red lines from 11:00 20 September, and yellow lines from 23:13 20 September. During this event the sea surface temperature stayed relatively constant at ~ 19°C.

The red line in figure 3.10 shows a nocturnal boundary layer consisting of a surface layer (0-250 m), residual layer (250-2000 m), and the top of the boundary layer and free troposphere interface (~2000 m) on 20 September. From figure 3.8, the dry air that entered the surface layer resulted in a water vapour mass mixing ratio of 0.0055 kg/kg at its lowest value. There are two possible reasons to explain a decrease in surface specific humidity. First, an air parcel originating in the free troposphere mixed with the air at the surface. The other possibility is that once the nocturnal boundary layer became a well-mixed boundary layer, the air from the residual layer mixed with the surface air, creating a mixed parcel with specific humidity of 0.0055 kg/kg.

Potential temperature is useful because it can be used to determine the stability of the atmosphere, where an increase in potential temperature with height shows a stable atmosphere with no rising air and a decrease in potential temperature with height shows an unstable atmosphere with rising air. Figure 3.10b shows that 4 hours before the event, the atmosphere was stable with no rising air in the surface and residual layers. By the end of the event, (yellow line), the surface and residual layers had combined into a single, well-mixed layer up to 2 km. The potential temperature profiles show that subsidence occurred on the previous day, indicated by the decrease in the values (blue line to red line) in the free troposphere. Subsidence over night the day before the event could have provided the boundary layer with precursor gases. A clean

marine boundary layer in the previous day from free tropospheric subsidence would have remained clean when it transitioned into a nocturnal boundary layer because separation from surface emissions created favourable conditions for nucleation in the morning of 20 September. The potential temperature profile in the free troposphere (above 2 km) remained unchanged throughout the event, suggesting that the interface between the boundary layer and free troposphere did not change and that subsidence into the boundary layer from above was unlikely. This suggests that although the free troposphere may have provided some of the necessary gases for nucleation, the nucleation most likely did not occur in the free troposphere.

Sanchez et al. 2018 and Covert et al. 1996 observed inversions separating the marine boundary layer and the free troposphere but did not mention any inversions present in the marine boundary layer, as observed in our study, where an inversion present at the surface before the event likely mimicked the marine boundary layer and free troposphere inversion. Sanchez et al. 2018 also observed that during the NAAMES1 study, the colder temperatures and lower particle concentration that occurred in November could support nucleation in the marine boundary layer rather than the free troposphere. Since the small particle appearance and growth event took place at the end of September the results found in this thesis could be consistent with the results of newly formed particles in the NAAMES1 study given that they both occurred in the Fall months.

The two temperature inversions at 250 m and 1250 m in figure 3.10a show the lower one separating the surface layer and residual layer, and the second inversion separating the marine boundary layer from the free troposphere. With the separation of the surface layer and the residual layer, the air in the residual layer would be uninfluenced from surface particle emissions

resulting in a lower condensation sink. The air subsiding from the free troposphere overnight before the event would have provided the precursor gases needed to nucleate particles and the overnight surface inversion would have prevented particles from being added to the upper boundary layer, creating a clean environment in the residual layer. Figure 3.10 shows the surface temperature inversion present 4 hours before the start of the event (8 am local time) that disappeared as the day progressed due to the disappearance of the nocturnal boundary layer by surface heating. Nucleation could have occurred in the residual layer after sunrise at 7 am local time. As the temperature inversion disappeared, the air mass containing the nucleated particles would have mixed with the surface layer which could have also contributed to gases needed to grow the aerosols.

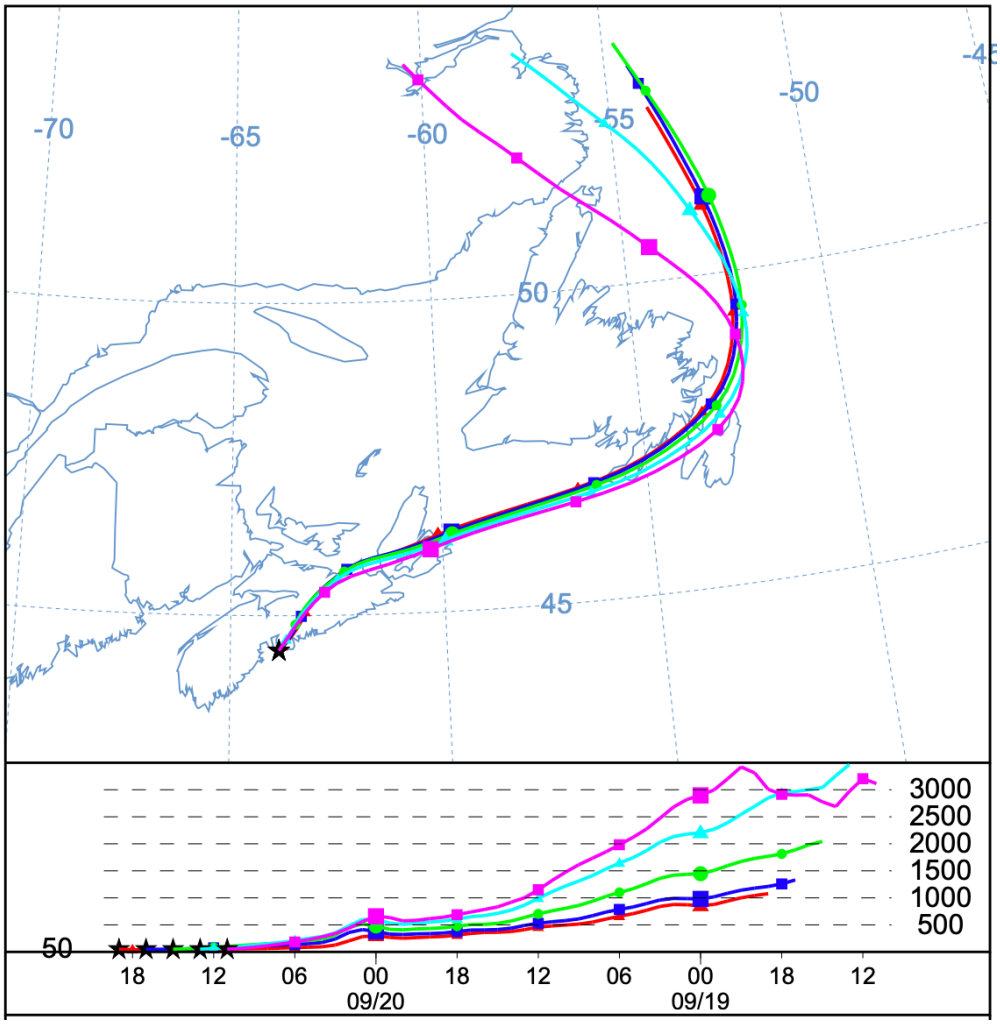

Figure 3.11: NOAA HYSPLIT model output for the backward trajectory of the air parcel in UTC associated with the appearance and growth of small particles event (Stein et. al, 2015).

The NOAA HYSPLIT back trajectory model was also run to simulate the origin of the air parcel (figure 3.11). The backward trajectory analysis shows the air parcel originating at around 500 m altitude on 20 September and over the ocean in the previous day's boundary layer. The trajectories also show the air parcel subsiding from the free troposphere on 19 September at night, which could contribute to a clean residual layer with the necessary precursor gases for nucleation to occur. The backward trajectory along with the vertical profile of potential

temperature confirm that there was free tropospheric subsidence into the boundary layer late on 19 September. Further downward mixing also occurred on 20 September corresponding to the time when the nocturnal boundary layer would have transitioned into the mixed boundary layer.

Figure 3.7 shows that the small particles grew from 10 nm to 30 nm (20 nm) over 4 hours, giving an estimated growth rate of 5 nm $hour^{-1}$. Extrapolating from the lower size limit of the SMPS (10.6 nm), it is estimated that the nucleation of 1 nm particles occurred at approximately 10 am local time (13 UTC), 2 hours before the particles were observed on the ship, when the air parcel was close to the surface over a forested part of Nova Scotia. At this time the air parcel was over forests, farms, and Halifax, along with marine emissions and subsidence from the free troposphere on the previous day, all which could have contributed precursor gases for nucleation. From this, the 10 nm sized particles appeared to originate in the MBL before the air mixed down to the ship and continued to grow from the nucleation mode to the Aitken mode at 30 nm. The timing of our event is consistent with observations by Kulmala et al. 2001, who found that all of the nucleation events observed in Southern Finland occurred when the boundary layer transitioned from the stable nocturnal boundary layer to a convective well-mixed boundary layer. At that surface site, nucleation is observed when turbulence associated with this transition allows increased mixing of nascent particle clusters, condensable vapours and temperature between the layers, resulting in a sudden decrease in the aerosol concentration with dilution, which favors new particle formation and aerosol growth to detectable sizes (Nilsson et al. 2001; Kulmala et al. 2001). All of these factors could have contributed to the event described here.

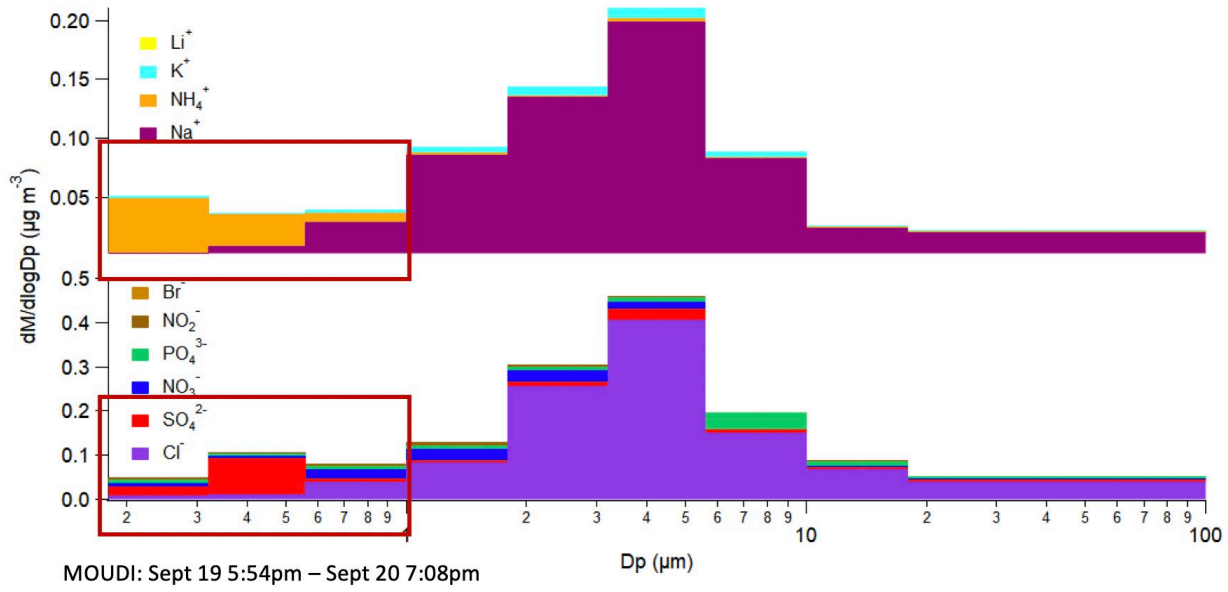

Figure 3.12: MOUDI mass concentration for the appearance and growth of small particles event. The smallest particles (red box) are dominated by ammonium and sulfate.

Figure 3.12 shows the size-resolved mass concentration of different ions during the time of the appearance and growth of small particles event. The chemical composition of the particles during this time was dominated by sodium chloride in the coarse mode which is expected for marine ambient air. The red box in figure 3.12 also shows the accumulation mode dominated by ammonium sulfate. Although the MOUDI only measures particles > 200 nm, the presence of ammonium and sulfate in the accumulation mode suggests that they may have also contributed to the nucleation mode, which would be consistent with our understanding of nucleation, where sulfate has been observed to play an important role in the formation and growth of particles (Kulmala et al. 2013; Kulmala et al. 2014). Along with sulfates and ammonia, VOCs are also important contributors to the nucleation and growth of particles and can be emitted from continental (Kulmala et al. 2001) and marine regions (Croft et al. 2019). Figure 3.11 shows the

air parcel passing over forested areas of Nova Scotia, farm lands near Truro and Halifax, all possible sources of condensable VOCs.

In addition to sulfuric acid, ammonia, VOCs, and amines playing important roles in aerosol nucleation, recent studies of coastal environments have also observed iodine to play an important role in aerosol nucleation. Iodine is naturally produced by macroalgae species when exposed to the atmosphere and has been observed in seaweed rich coastal areas (Allan et al. 2015). This phenomenon of iodine contributing to new particle formation has been measured and modeled in lower latitudes and in coastal regions (O'Dowd et al. 2002). Since the ship was near St. Margaret's Bay, a rocky coastal area with kelp off the coast of Nova Scotia, when the 10 nm particles were observed, it is possible that iodine was the source of particle nucleation and growth. However, iodine was most likely not the source of particle nucleation because the growth rate shows the particles nucleating about 2 hours before they were seen by the ship and the air parcel had not reached the coast yet. The iodine emissions could have contributed to the growth of the already nucleated particles.

To summarize, a clean boundary layer the previous day would have been possible by free troposphere subsidence that occurred 16 hours before the start of the event. Since this subsidence occurred sometime between 8 pm and 7 am local time a clean layer continued in the residual layer overnight due to a surface inversion preventing particles emitted from the surface from entering. When the sun rose, the nocturnal boundary layer transitioned into a mixed boundary layer allowing for the residual layer and the surface layer to mix. Gases from these layers such as VOCs, sulfates, ammonia, and potentially iodine emitted from the forests, farms, Halifax, and

coastal macroalgae species, along with a low condensation sink in the clean boundary layer could have contributed to the nucleation of the particles that were ultimately observed at the ship. The abundance of precursor gases, the dilution of the particle concentration from the surface, a residual layer transitioning into a mixed boundary layer, and the appearance of the sun, all simultaneously allowed for nucleation to occur and growth of these newly formed particles.

3.4 Growth Only Event

The particle growth event occurred on 16:00 23 September 2018 UTC and lasted until 00:00 24 September 2018 UTC, during which an existing 40 nm mode aerosol grew to 75 nm. The meteorological observations showed that the atmosphere was partly cloudy for the entire duration of the event. Figure 3.13 shows the total number concentration on the top and the particle size distribution time series on the bottom. The figure shows an existing background size distribution that peaks in the Aitken mode and then shifted to a larger Aitken mode throughout the event. The average total number concentration during this event was 1335 cm^{-3}±244 cm^{-3} and was relatively steady throughout the whole event. This is in contrast to the appearance of small particles and growth event where the particle concentrations increased before the start of the event.

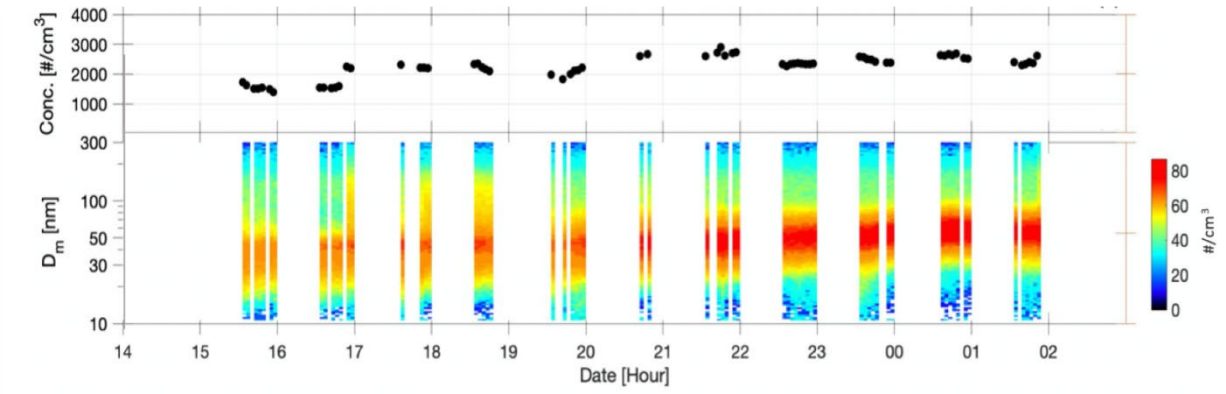

Figure 3.13: Total number concentration, panel (a), and particle size distribution during the growth event, panel (b).

Similar to the small particle appearance and growth event, the origin of the air parcel that caused the growth of Aitken mode particles was investigated to determine the source of the aerosols. Figure 3.14 shows the meteorology time series variables of pressure, relative humidity, specific humidity, and temperature. Starting with pressure, there appears to not be a significant change in pressure during the time of the event but midway through the event and after the event the pressure was rising, which indicated another period of subsidence. The relative and specific humidity increased during the event which could indicate mixing occurred in the marine boundary layer.

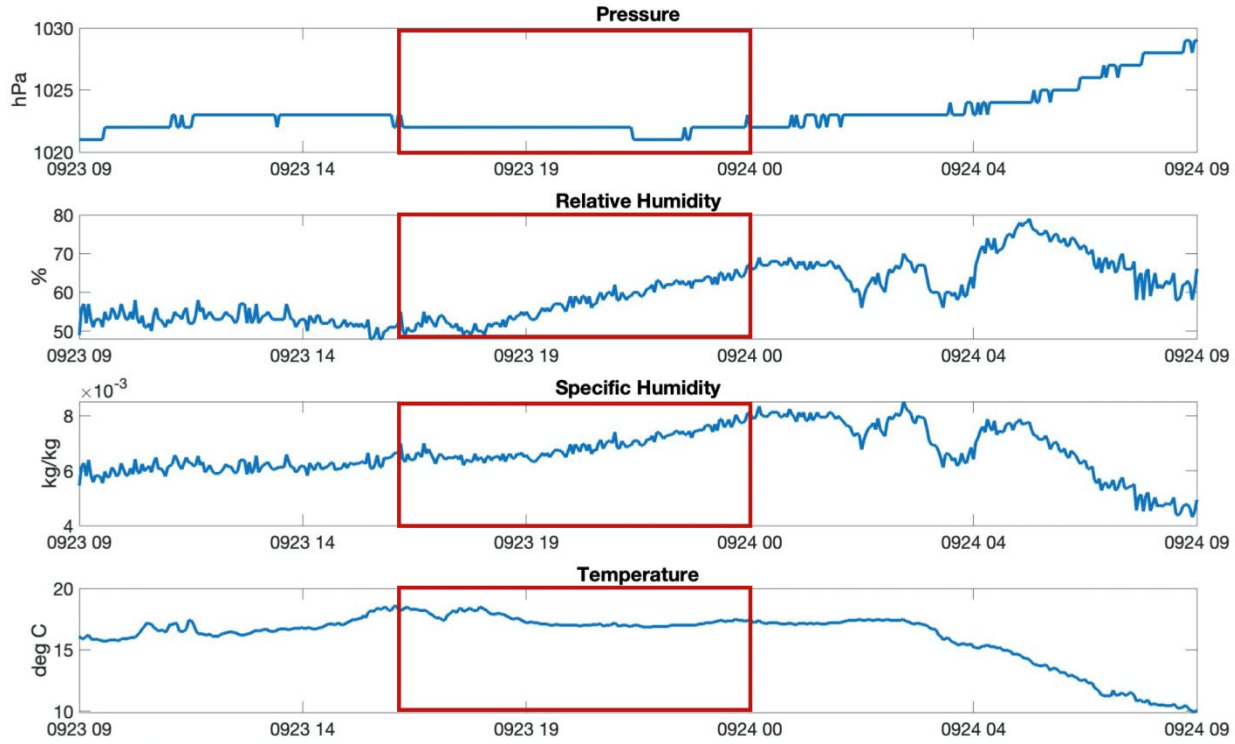

Figure 3.14: The time series plot of pressure, relative humidity, specific humidity, and temperature during the particle growth event where the time of the actual event occurred is enclosed in the red box.

To further investigate the origin of this air parcel and therefore why these particles grew about 35 nm in size the vertical profiles of temperature, potential temperature, and specific humidity were plotted in figure 3.15. Three radiosondes were released before, during, and close to the end of the event from the stern of the ship. The first radiosonde was released 5 hours before the start of the event at 11:14 23 September, the second radiosonde was released an hour after the start of the event at 17:11 23 September, and the last radiosonde released at 23:14 23 September 1 hour before the end of the event. The next radiosonde was not released until 25 September and is therefore not relevant for this event.

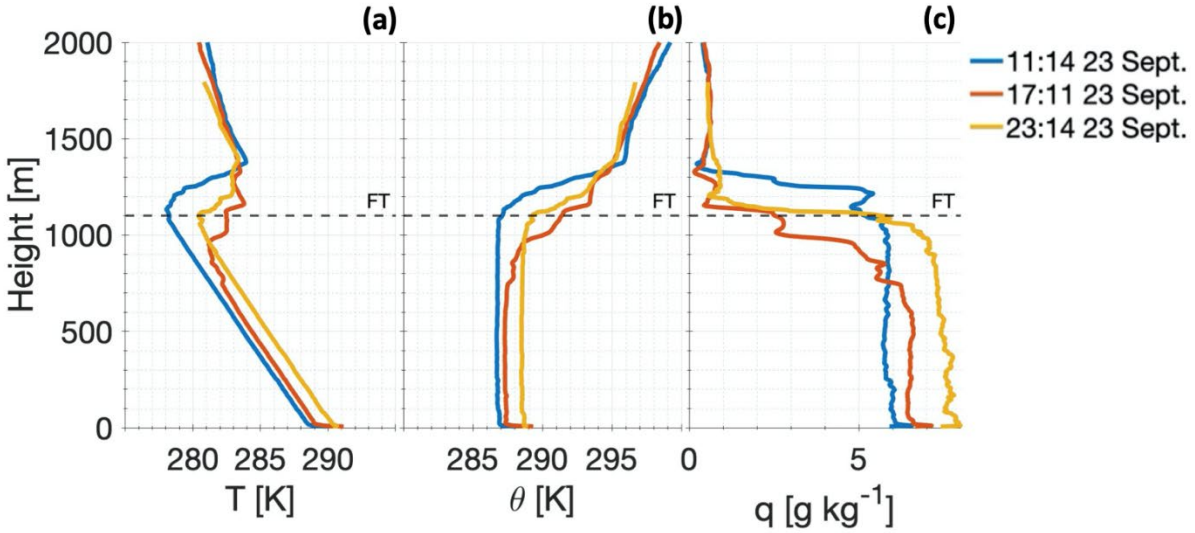

Figure 3.15: Vertical profiles of temperature, panel (a), potential temperature, panel (b), and specific humidity, panel (c) during the growth event: 11:14 23 September (blue line), 17:11 23 September (red line), and 23:14 23 September (yellow line). During this event the sea surface temperature stayed relatively constant at ~ 19°C.

From figure 3.15, the top of the marine boundary layer is somewhere around 1100 m with the temperature decreasing with height and the specific humidity remaining constant with height in the marine boundary layer before the start of the event. Comparing figures 3.14 and 3.15, the specific humidity at the surface before the event was around 0.006 kg/kg and relatively constant throughout the entire boundary layer which is consistent in the two figures. Figure 3.15 also shows that potential temperature and specific humidity were constant with height in the boundary layer throughout the event which was likely due to a well-mixed boundary layer. The potential temperature started out constant with height in the marine boundary layer and increased with height above the layer. This implies that there was no rising air present in the marine

boundary layer throughout the event which is consistent with the theory that the air stayed in the well mixed marine boundary layer leading up to the event.

The NOAA HYSPLIT back trajectory model was also used to investigate the origins of the air parcel, with the results shown in figure 3.16. Panel (a) shows the backward trajectory analysis for the air parcel at the start of the event and panel (b) shows the back trajectory for the air parcel at the end of the event. This figure shows that 48 hours before the start of the particle growth event this air parcel was in the free troposphere and over northern Ontario and Quebec. The air parcel started to descend into the marine boundary layer around 24 hours before the particle growth event was observed and by 16 hours before the event the air parcel was 500 m above the surface and descending. This supports the evidence that the air parcel spent the majority of the time leading up to the event in the marine boundary layer. The backward trajectories also show the possibility of these particles nucleating in the free troposphere before descending and growing, most likely by the VOCs emitted from the boreal forests over Quebec and Atlantic Canada.

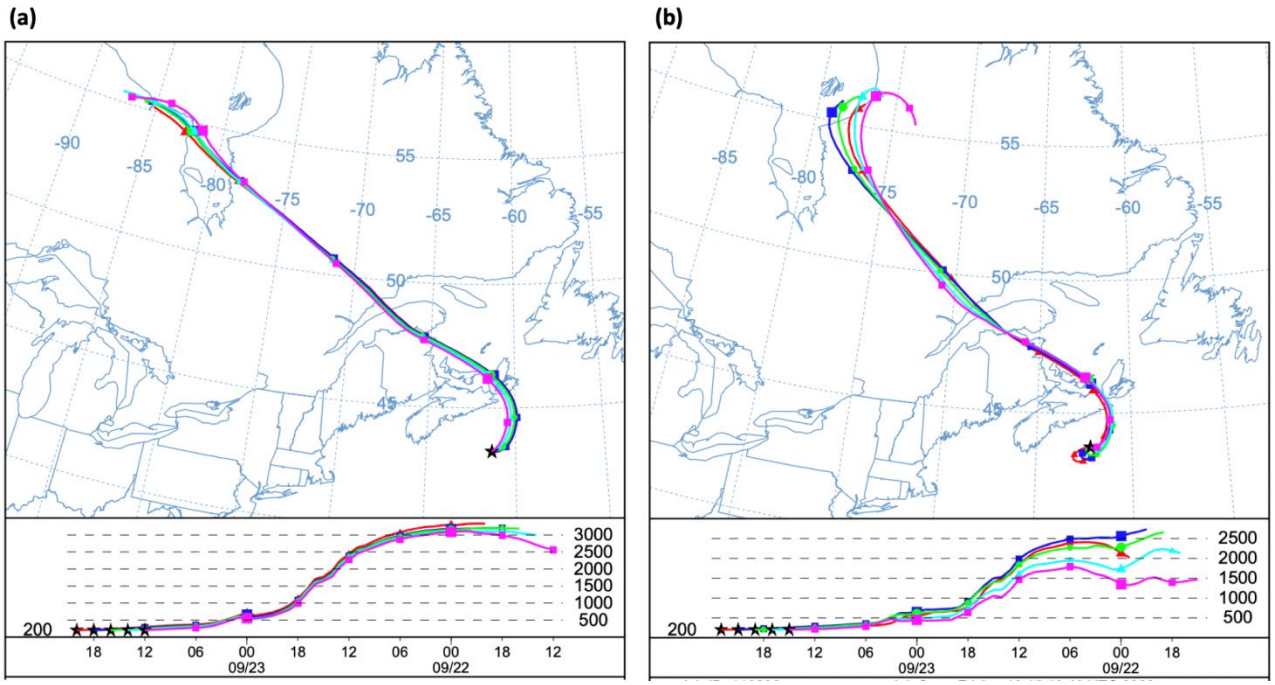

Figure 3.16: NOAA HYSPLIT back trajectory model at the start of the particle growth event in panel (a) and the back trajectory at the end of the event in panel (b) (Stein et. al, 2015).

Aerosol growth in marine environments is often attributed to cloud processing. Growth by cloud processing can occur through coagulation, condensation, and aqueous oxidation of sulfate (Harris et al. 2014). During the duration of the growth event, the sky was partly cloudy, which makes cloud processing a possible explanation for the observed growth. It is possible that particles in the middle to top of the boundary layer were cloud processed and brought to the surface through the well mixed boundary layer by cloud outflows. This would have modified the existing background aerosols by growing Aitken mode particles to accumulation mode particles, resulting in a bimodal size distribution (Hoppel et al. 1985). Bates et al. 1998 studied the aerosol physical properties and processing in the lower marine boundary layer through two studies, ACE-1 and ACE-2, and found that that a well-defined Aitken mode occurs due to cloud processing. Growth by cloud processing normally occurs by SO_2 oxidation in cloud droplets. The

cloud droplets on the edge of the cloud would then evaporate and exit the cloud through the cloud outflows, resulting in larger residual particles than those that entered the cloud. The scattered clouds from the passing front could explain the growth of Aitken mode particles observed on the ship. However, when cloud processing occurs, the accumulation mode also grows (Hoppel et al. 1985) which is inconsistent with the observations. Figure 3.13 shows the small concentration of 150 nm accumulation mode particles remaining constant at 150 nm throughout the event. There is no significant sulfate mass in the accumulation mode, therefore, it is unlikely that cloud processing could explain the observations during the particle growth event.

Another possible explanation for the growth of these aerosols is the direct condensation of low volatility gases onto existing aerosols. The condensation most likely occurred through direct condensation of low volatility gases including marine VOCs (Croft et al. 2019). Satellite images showed that chlorophyll a was higher off the coast of Nova Scotia than in the open ocean ("NASA Earth Observatory" 2020), suggesting that biological activity was high near the ship and that the ocean was a potential source of VOCs. Mungall et al. 2017 also suggests an abiotic source of VOCs through heterogeneous chemistry at the ocean surface, where the study found high levels of organic acids not correlated with DMS emission. By the end of the event the backward trajectories show the air increasingly influenced by the ocean surface, allowing more opportunity for marine organic emissions to condense on the Aitken mode particles. Another possible reason for the growth of these aerosols could include the nucleation and growth of these particles in the free troposphere through the emission of VOCs from the boreal forests in Eastern Canada. There could also be influence from marine emissions that further aided in the growth of the Aitken mode particles since the air parcel also spent time over the Atlantic Ocean. Therefore,

the direct condensation of marine organics, along with the time spent over the boreal forests, were most likely sources of the growth of the Aitken mode particles.

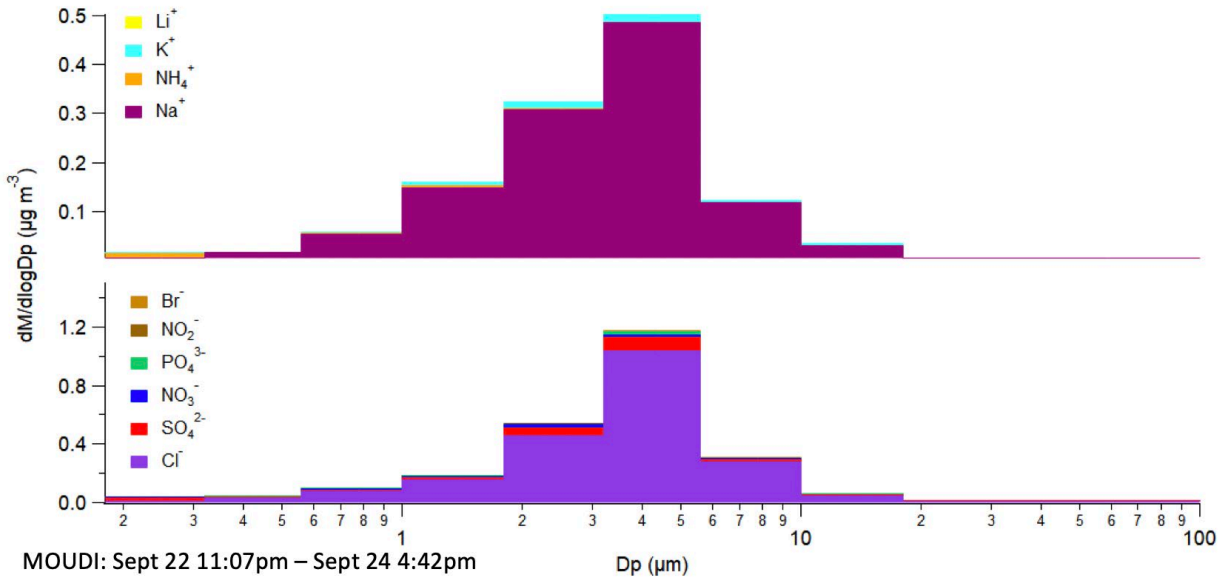

Figure 3.17: MOUDI data during the time of the particle growth event.

The size-resolved chemical composition measured by the MOUDI is shown in figure 3.17. As with all the samples, sea salt dominates the mass concentration in the coarse mode for marine air. However, there is very little mass in the accumulation mode, including secondary components such as ammonium and sulfate. These components appear to be dominating the lowest size bin of 200 nm but compared to the small particle appearance and growth event, their mass contribution is small. This would be consistent with VOCs being the primary condensing species since they would not have been detected by the MOUDI.

Chapter 4: Conclusions

Aerosol chemical and physical properties were measured as part of the C-FOG study on board the R/V Hugh R. Sharp off the coast of the NE USA and Atlantic Canada between 31 August and 07 October 2018. This study characterized the aerosol properties, sources and processing for eight distinct times that highlight aerosol growth in the marine boundary layer, processed marine aerosols and harbour emissions.

Processed marine aerosol size distributions were observed to have distinct Aitken and accumulation mode, thought to form through cloud processing. These bimodal observations are consistent with past studies in this region. In one period, however, a single accumulation mode was observed after the dissipation of a stationary front along with precipitation, which was interpreted as an aged air mass in which smaller particles were lost through condensation, coagulation, and/or wet scavenging. The importance of cloud processing on the physical and chemical properties of marine aerosols has long been studied (Hoppel et al. 1985), although more recent work has suggested that other processes can contribute (Hudson et al. 2015). Assuming the particles were composed of ammonium sulfate and using Kohler theory (Köhler 1936), the observed Hoppel minimum of 80 nm – 100 nm would correspond to in-cloud supersaturations of 0.16% to 0.21%, consistent with marine stratocumulus clouds (Hoppel et al. 1985). Our results suggest that clouds associated with a frontal passage contributed to the bimodal aerosol distribution for a 6 to 8 September case. The distributions had a persistent Aitken-mode modal diameter at 50 nm while the accumulation mode peak shifted to larger sizes, supporting cloud processing as the cause of the observed bimodal distribution.

The St. John's harbour and city centre are entirely surrounded by hills. This topography limits mixing from above to dilute the air, sometimes causing the build-up of particulate matter from emissions from the harbour and city centre. In contrast, Halifax harbour is more spread out with less abrupt topography, resulting in easier dilution with other air masses, which can lower aerosol concentrations and enable a more prominent influence of transported aerosols. It should be noted that the sampling in St. John's lasted for one day and the sampling in Halifax lasted for two days. With these small sample sizes it is difficult to provide general comparisons or conclusions on the residents' aerosol exposure.

A burst of 10 nm particles was observed on 20 September 2018 that then grew to 30 nm in diameter. Analysis of the meteorological conditions suggested that these particles formed in the residual layer shortly after sunrise when mixing occurred between the surface and residual layers and photochemical reactions could occur. This upper portion of the boundary layer had been influenced by large-scale subsidence from the free troposphere the previous day as well as surface emissions from the ocean, both of which could have provided condensable vapours that would have contributed to the formation and growth of the 10 nm particles. Additional condensable vapours emitted by forested, farm and urban regions while the parcel travelled over Nova Scotia could have also contributed to the observed aerosols and their subsequent growth. Overall, the large scale movement of the air parcel suggests that these 10 nm particles were formed within the boundary layer, which would be more typical of the summertime Arctic MBL (Collins et al. 2017). However, it is possible that the particles were formed in the free troposphere and entrained into the boundary layer in the few hours prior to our observations.

Covert et al. 1996 and Pirjola et al. 2000 discuss the fact that nucleation is prominent in the free troposphere where the air does not contain many aerosols and large amounts of the precursor gases are available. These conditions arise because of the temperature inversion that prevents air from the marine boundary layer mixing into the free troposphere. Recent modelling work has shown large concentrations of nucleation mode particles near/above the MBL at ~1 km (Croft et al. submitted), where the condensation sink is weak/low. Further studies are needed since the level of the atmosphere (FT or MBL) where nucleation occurs is still uncertain and has been shown to be dependent on the given atmospheric conditions.

A second growth event was observed on 23 September 2018, where 40 nm particles grew to 70 nm in diameter. The two possible reasons for the growth of these particles are growth through cloud processing and growth through direct condensation of vapours. Cloud processing was mostly likely not the cause of the growth because only the Aitken mode particles grew and not the accumulation mode. Also, there was a lack of sulphate in the accumulation mode, which further shows that aerosol growth by aqueous-phase sulphate in cloud droplets did not occur. In this event the air mass had spent more time over the ocean in the preceding 12-24 hours. As a result, the likely growth of the aerosols was through direct condensation with contributors to the observed growth and secondary aerosol mass could include condensable organic vapours originating from more local biological or abiotic sources in the surface ocean, as well as the more distant boreal forest of Quebec.

Both of the observed cases of particle growth in the MBL point to the importance of condensable vapours on controlling the aerosol size distribution and the need to understand the sources of

these vapours. Vapours contributing to the observed growth likely included sulphate, ammonium, alkyl amine and organic compounds, most of whose sources remain poorly characterized in coastal and more open waters. In both of these cases, the air was potentially influenced by continental emissions, so that it is not possible to attribute the growth entirely to oceanic emissions. The ultimate contribution of these growing particles on fog and cloud droplets is marginal. If the aerosols were as hygroscopic as ammonium sulphate, then the 70 nm particles observed during the growth-only event would activate into cloud droplets at 0.24% supersaturation, which is not unreasonable for marine clouds. However, the smaller particles observed during the small particle appearance and growth event, the presence of less-hygroscopic organic compounds as suggested by the MOUDI analysis and the lower supersaturations expected during fog, would all require more favourable conditions for droplet activation. Nevertheless, further atmospheric processing through growth and chemical ageing would improve their likelihood for affecting cloud and fog properties.

Nucleation and growth by condensation are complicated processes and there are many contributors to these processes that are uncertain. More research on the processes of the nucleation and growth of these newly formed particles is needed to understand how it occurs in different environments and what atmospheric processes contribute to these processes. Measurements such as the vertical profiles of temperature, potential temperature, and specific humidity, along with vertical profiles of total particle concentration and particle size distributions at multiple land sites would be useful in determining how particles change over time. These measurements would also be useful to determine spatial variation of particle concentration and

sizes, since during this campaign our observations only provide a snapshot in time over one column of the atmosphere and therefore estimations on the air parcel's path were made.

Further analysis on the processed marine aerosols, harbour air, and the two particle growth events can be done by analyzing their CCN activity. The CCN analysis of the processed marine air would be useful to speculate on how theses aerosols contribute to the indirect effect. The CCN analysis could also provide insight on the chemical composition of the processed marine aerosols. This could also help our understanding of the origin of these aerosols as well as the processes that these aerosols underwent during their time in the MBL. The CCN analysis of the harbour air in Halifax and St. John's can provide insight on the chemical composition of these aerosols and therefore what aerosol source in the harbours and downtown area contribute the most to the air quality. Finally, CCN activity and hygroscopicity of the two growth events would provide understanding on how and why these particles grew and the source of the particles and potential precursors used in the growing of these particles. The CCN activity can also be used to determine how much these particles contributed to the indirect effect.

Looking back on the experiment, there were a few limitations and therefore things that I would change if there were to be another cruise. First, I would have changed how the inlet sampled the ambient air. During this cruise the inlet was set up to alternate between the interstitial line and the droplet line approximately every thirty minutes. I would set up the inlet so that the interstitial line was sampling continuously during the cruise, expect for when there was fog present, then the inlet would switch between the lines every thirty minutes to gain insight on what mode of particles contributed to the fog. Second, I would have placed the inlet more towards the front of

the ship in order to further try to eliminate the aerosols exposure to the ship emissions. With the layout of the ship used during this cruise that was not possible and the inlet was placed in the best position available. Thirdly, the ship stayed within ~275 km of the shore line and therefore the marine aerosols saw most likely had some continental influence and not solely marine aerosols. Some CCN analysis was done for the work in this thesis but some problems arose when trying to determine if the CCNC was counting correctly. To try and prevent this in the future, I would suggest calibrating the instrument at least once a week in order to see how efficiently it was counting throughout the cruise. More cruises during the same season as this one as well as during other seasons would further provide useful information on the physical properties of aerosols and the processes affecting them. Since there was only one small particle appearance and growth event and one growth event comparisons were done with other studies instead of events within the same study. Sampling more events at the same location could provide insight on if the processes observed in this study occur frequently and if the processes that produced these events occurred in the same way. Also, sampling the same locations during different seasons would provide insight on how the processes affecting the aerosols change. For example, will nucleation only occur in the MBL during the fall and winter months and in the free troposphere during the spring and summer months due to different processes occurring during different seasons? Finally, comparison of these result to model output would also be useful to see how well the model simulates the observations. Also, this analysis could help improve models by providing information on how the observed particles nucleated and grew and the proposed processes that influenced these particles. In conclusion, the results from these observations were really exciting and provide a glimpse of what is happening with processes affecting aerosols in

the boundary layer and additional research will be needed to fully understand these processes and their ultimate effect on the aerosols in the atmosphere.

References

Allan, J. D., P. I. Williams, J. Najera, J. D. Whitehead, M. J. Flynn, J. W. Taylor, D. Liu, et al. 2015. "Iodine Observed in New Particle Formation Events in the Arctic Atmosphere during ACCACIA." *Atmospheric Chemistry and Physics* 15 (10): 5599–5609. https://doi.org/10.5194/acp-15-5599-2015.

"AR5 Climate Change 2013: The Physical Science Basis — IPCC." n.d. Accessed March 9, 2020. https://www.ipcc.ch/report/ar5/wg1/.

Bates, Timothy S., Vladimir N. Kapustin, Patricia K. Quinn, David S. Covert, Derek J. Coffman, Celine Mari, Philip A. Durkee, Warren J. De Bruyn, and Eric S. Saltzman. 1998. "Processes Controlling the Distribution of Aerosol Particles in the Lower Marine Boundary Layer during the First Aerosol Characterization Experiment (ACE 1)." *Journal of Geophysical Research: Atmospheres* 103 (D13): 16369–83. https://doi.org/10.1029/97JD03720.

Bates, Timothy S., Patricia K. Quinn, David S. Covert, Derek J. Coffman, James E. Johnson, and Alfred Wiedensohler. 2000. "Aerosol Physical Properties and Processes in the Lower Marine Boundary Layer: A Comparison of Shipboard Sub-Micron Data from ACE-1 and ACE-2." *Tellus B* 52 (2): 258–72. https://doi.org/10.1034/j.1600-0889.2000.00021.x.

Butz, André, Anna Solvejg Dinger, Nicole Bobrowski, Julian Kostinek, Lukas Fieber, Constanze Fischerkeller, Giovanni Bruno Giuffrida, et al. 2017. "Remote Sensing of Volcanic CO_2, HF, HCl, SO_2, and BrO in the Downwind Plume of Mt. Etna." *Atmospheric Measurement Techniques* 10 (1): 1–14. https://doi.org/10.5194/amt-10-1-2017.

Charlson, R. J., S. E. Schwartz, J. M. Hales, R. D. Cess, J. A. Coakley, J. E. Hansen, and D. J. Hofmann. 1992. “Climate Forcing by Anthropogenic Aerosols.” *Science* 255 (5043): 423–30. https://doi.org/10.1126/science.255.5043.423.

Collins, Douglas B., Julia Burkart, Rachel Y.-W. Chang, Martine Lizotte, Aude Boivin-Rioux, Marjolaine Blais, Emma L. Mungall, et al. 2017. “Frequent Ultrafine Particle Formation and Growth in Canadian Arctic Marine and Coastal Environments.” *Atmospheric Chemistry and Physics* 17 (21): 13119–38. https://doi.org/10.5194/acp-17-13119-2017.

Covert, D. S., V. N. Kapustin, T. S. Bates, and P. K. Quinn. 1996. “Physical Properties of Marine Boundary Layer Aerosol Particles of the Mid-Pacific in Relation to Sources and Meteorological Transport.” *Journal of Geophysical Research: Atmospheres* 101 (D3): 6919–30. https://doi.org/10.1029/95JD03068.

Covert, David S., Vladimir N. Kapustin, Patricia K. Quinn, and Timothy S. Bates. 1992. “New Particle Formation in the Marine Boundary Layer.” *Journal of Geophysical Research: Atmospheres* 97 (D18): 20581–89. https://doi.org/10.1029/92JD02074.

Croft, Betty, Randall V. Martin, W. Richard Leaitch, Julia Burkart, Rachel Y.-W. Chang, Douglas B. Collins, Patrick L. Hayes, et al. 2019. “Arctic Marine Secondary Organic Aerosol Contributes Significantly to Summertime Particle Size Distributions in the Canadian Arctic Archipelago.” *Atmospheric Chemistry and Physics* 19 (5): 2787–2812. https://doi.org/10.5194/acp-19-2787-2019.

Ervens, B., B. Turpin, and R. Weber. 2011. “Secondary Organic Aerosol Formation in Cloud Droplets and Aqueous Particles (AqSOA): A Review of Laboratory, Field and Model Studies.” *Atmospheric Chemistry and Physics* 11 (November). https://doi.org/10.5194/acp-11-11069-2011.

Fernando HJS, Gultepe I, Dorman C, Pardyjak E, Wang Q, Hoch SW, Richter D, Creegan E, Gaberšek S, Bullock T, Hocut C, Chang R, Alappattu D, Dimitrova R, Flagg D, Grachev A, Krishnamurthy R, Singh DK, Lozovatsky I, Nagare B, Sharma A, Wagh S, Wainwright C, Wroblewski M, Yamaguchi R, Bardoel S, Coppersmith RS, Chisholm N, Gonzalez E, Gunawardena N, Hyde O, Morrison T, Olson A, Perelet A, Perrie W, Wang S, Wauer B. n.d. "C-FOG: Life of Coastal Fog."

Fitzgerald, James W. 1991. "Marine Aerosols: A Review." *Atmospheric Environment. Part A. General Topics* 25 (3): 533–45. https://doi.org/10.1016/0960-1686(91)90050-H.

Gantt, B., and N. Meskhidze. 2013. "The Physical and Chemical Characteristics of Marine Primary Organic Aerosol: A Review." *Atmospheric Chemistry and Physics* 13 (8): 3979–96. https://doi.org/10.5194/acp-13-3979-2013.

Gaston, Cassandra J., Hiroshi Furutani, Sergio A. Guazzotti, Keith R. Coffee, Timothy S. Bates, Patricia K. Quinn, Lihini I. Aluwihare, B. Gregory Mitchell, and Kimberly A. Prather. 2011. "Unique Ocean-Derived Particles Serve as a Proxy for Changes in Ocean Chemistry." *Journal of Geophysical Research: Atmospheres* 116 (D18). https://doi.org/10.1029/2010JD015289.

Grythe, H., J. Ström, R. Krejci, P. Quinn, and A. Stohl. 2014. "A Review of Sea-Spray Aerosol Source Functions Using a Large Global Set of Sea Salt Aerosol Concentration Measurements." *Atmospheric Chemistry and Physics* 14 (3): 1277–97. https://doi.org/10.5194/acp-14-1277-2014.

Harris, E., B. Sinha, D. van Pinxteren, J. Schneider, L. Poulain, J. Collett, B. D'Anna, et al. 2014. "In-Cloud Sulfate Addition to Single Particles Resolved with Sulfur Isotope

Analysis during HCCT-2010." *Atmospheric Chemistry and Physics* 14 (8): 4219–35. https://doi.org/10.5194/acp-14-4219-2014.

Haywood, James, and Olivier Boucher. 2000. "Estimates of the Direct and Indirect Radiative Forcing Due to Tropospheric Aerosols: A Review." *Reviews of Geophysics* 38 (4): 513–43. https://doi.org/10.1029/1999RG000078.

Hoppel, William A., James W. Fitzgerald, and Reginald E. Larson. 1985. "Aerosol Size Distributions in Air Masses Advecting off the East Coast of the United States." *Journal of Geophysical Research: Atmospheres* 90 (D1): 2365–79. https://doi.org/10.1029/JD090iD01p02365.

Hudson, James G., Stephen Noble, and Samantha Tabor. 2015. "Cloud Supersaturations from CCN Spectra Hoppel Minima." *Journal of Geophysical Research: Atmospheres* 120 (8): 3436–52. https://doi.org/10.1002/2014JD022669.

Jacob, Daniel J. 1999. *Introduction to Atmospheric Chemistry*. Princeton University Press.

Köhler, Hilding. 1936. "The Nucleus in and the Growth of Hygroscopic Droplets." *Transactions of the Faraday Society* 32 (0): 1152–61. https://doi.org/10.1039/TF9363201152.

Kremser, Stefanie, Larry W. Thomason, Marc von Hobe, Markus Hermann, Terry Deshler, Claudia Timmreck, Matthew Toohey, et al. 2016. "Stratospheric Aerosol—Observations, Processes, and Impact on Climate." *Reviews of Geophysics* 54 (2): 278–335. https://doi.org/10.1002/2015RG000511.

Kulmala, M., K. Hämeri, P. P. Aalto, J. M. Mäkelä, L. Pirjola, E. Douglas Nilsson, G. Buzorius, et al. 2001. "Overview of the International Project on Biogenic Aerosol Formation in the Boreal Forest (BIOFOR)." *Tellus B: Chemical and Physical Meteorology* 53 (4): 324–43. https://doi.org/10.3402/tellusb.v53i4.16601.

Kulmala, M., T. Petäjä, M. Ehn, J. Thornton, M. Sipilä, D.R. Worsnop, and V.-M. Kerminen. 2014. “Chemistry of Atmospheric Nucleation: On the Recent Advances on Precursor Characterization and Atmospheric Cluster Composition in Connection with Atmospheric New Particle Formation.” *Annual Review of Physical Chemistry* 65 (1): 21–37. https://doi.org/10.1146/annurev-physchem-040412-110014.

Kulmala, Markku, Jenni Kontkanen, Heikki Junninen, Katrianne Lehtipalo, Hanna E. Manninen, Tuomo Nieminen, Tuukka Petäjä, et al. 2013. “Direct Observations of Atmospheric Aerosol Nucleation.” *Science (New York, N.Y.)* 339 (6122): 943–46. https://doi.org/10.1126/science.1227385.

Lohmann, U., and J. Feichter. 2005. “Global Indirect Aerosol Effects: A Review.” *Atmospheric Chemistry and Physics* 5 (3): 715–37. https://doi.org/10.5194/acp-5-715-2005.

Lovelock, J. E., R. J. Maggs, and R. A. Rasmussen. 1972. “Atmospheric Dimethyl Sulphide and the Natural Sulphur Cycle.” *Nature* 237 (5356): 452–53. https://doi.org/10.1038/237452a0.

Matteo, Rinaldi, Stefano Decesari, Emanuela Finessi, Lara Giulianelli, C. Carbone, Fuzzi Sandro, Colin O’Dowd, Darius Ceburnis, and Maria Facchini. 2010. “Primary and Secondary Organic Marine Aerosol and Oceanic Biological Activity: Recent Results and New Perspectives for Future Studies.” *Advances in Meteorology* 10 (May). https://doi.org/10.1155/2010/310682.

Mungall, Emma L., Jonathan P. D. Abbatt, Jeremy J. B. Wentzell, Alex K. Y. Lee, Jennie L. Thomas, Marjolaine Blais, Michel Gosselin, et al. 2017. “Microlayer Source of Oxygenated Volatile Organic Compounds in the Summertime Marine Arctic Boundary

Layer." *Proceedings of the National Academy of Sciences* 114 (24): 6203–8. https://doi.org/10.1073/pnas.1620571114.

"NASA Earth Observatory - Home." 2020. Text.Article. NASA Earth Observatory. June 2, 2020. https://earthobservatory.nasa.gov/.

Nilsson, E. D., U. Rannik, M. Kulmala, G. Buzorius, and C. D. O'Dowd. 2001. "Effects of Continental Boundary Layer Evolution, Convection, Turbulence and Entrainment, on Aerosol Formation." *Tellus B* 53 (4): 441–61. https://doi.org/10.1034/j.1600-0889.2001.530409.x.

O'Dowd, Colin, Jose Jimenez, Roya Bahreini, Richard Flagan, John Seinfeld, Kaarle Hämeri, Liisa Pirjola, Markku Kulmala, S Jennings, and Thorsten Hoffmann. 2002. "Marine Aerosol Formation from Biogenic Iodine Emissions." *Nature* 417 (July): 632–36. https://doi.org/10.1038/nature00775.

Ovadnevaite, Jurgita, Darius Ceburnis, Stephan Leinert, Manuel Dall'Osto, Manjula Canagaratna, Simon O'Doherty, Harald Berresheim, and Colin O'Dowd. 2014. "Submicron NE Atlantic Marine Aerosol Chemical Composition and Abundance: Seasonal Trends and Air Mass Categorization." *Journal of Geophysical Research: Atmospheres* 119 (20): 11,850-11,863. https://doi.org/10.1002/2013JD021330.

Pirjola, Liisa, Colin D. O'Dowd, Ian M. Brooks, and Markku Kulmala. 2000. "Can New Particle Formation Occur in the Clean Marine Boundary Layer?" *Journal of Geophysical Research: Atmospheres* 105 (D21): 26531–46. https://doi.org/10.1029/2000JD900310.

Place, Bryan K., Cora J. Young, Susan E. Ziegler, Kate A. Edwards, Leyla Salehpoor, and Trevor C. VandenBoer. 2018. "Passive Sampling Capabilities for Ultra-Trace Quantitation of Atmospheric Nitric Acid (HNO3) in Remote Environments."

Atmospheric Environment 191 (October): 360–69. https://doi.org/10.1016/j.atmosenv.2018.08.030.

Quinn, P., Derek Coffman, James Johnson, L. Upchurch, and T. Bates. 2017. "Small Fraction of Marine Cloud Condensation Nuclei Made up of Sea Spray Aerosol." *Nature Geoscience* 10 (August). https://doi.org/10.1038/ngeo3003.

Rosenfeld, Daniel, Yannian Zhu, Minghuai Wang, Youtong Zheng, Tom Goren, and Shaocai Yu. 2019. "Aerosol-Driven Droplet Concentrations Dominate Coverage and Water of Oceanic Low-Level Clouds." *Science* 363 (6427). https://doi.org/10.1126/science.aav0566.

Royalty, T. M., B. N. Phillips, K. W. Dawson, R. Reed, N. Meskhidze, and M. D. Petters. 2017. "Aerosol Properties Observed in the Subtropical North Pacific Boundary Layer." *Journal of Geophysical Research: Atmospheres* 122 (18): 9990-10,012. https://doi.org/10.1002/2017JD026897.

Sanchez, Kevin J., Chia-Li Chen, Lynn M. Russell, Raghu Betha, Jun Liu, Derek J. Price, Paola Massoli, et al. 2018. "Substantial Seasonal Contribution of Observed Biogenic Sulfate Particles to Cloud Condensation Nuclei." *Scientific Reports* 8 (1): 3235. https://doi.org/10.1038/s41598-018-21590-9.

Seinfeld, John H., and Spyros N. Pandis. 2016. *Atmospheric Chemistry and Physics*. Third. Hoboken, New Jersey: John Wiley & Sons Inc.

Stein, A. F., R. R. Draxler, G. D. Rolph, B. J. B. Stunder, M. D. Cohen, and F. Ngan. 2015. "NOAA's HYSPLIT Atmospheric Transport and Dispersion Modeling System." *Bulletin of the American Meteorological Society* 96 (12): 2059–77. https://doi.org/10.1175/BAMS-D-14-00110.1.

Twomey, S. 1991. “Aerosols, Clouds and Radiation.” *Atmospheric Environment. Part A. General Topics*, Symposium on Global Climatic Effects of Aerosols, 25 (11): 2435–42. https://doi.org/10.1016/0960-1686(91)90159-5.

Wallace, John M., and Peter V. Hobbs. 2006. *Atmospheric Science: An Introductory Survey*. Second. Elsevier Inc.

Wilson, Theodore W., Luis A. Ladino, Peter A. Alpert, Mark N. Breckels, Ian M. Brooks, Jo Browse, Susannah M. Burrows, et al. 2015. “A Marine Biogenic Source of Atmospheric Ice-Nucleating Particles.” *Nature* 525 (7568): 234–38. https://doi.org/10.1038/nature14986.

Zhang, Hongliang, Jianlin Hu, Michael Kleeman, and Qi Ying. 2014. “Source Apportionment of Sulfate and Nitrate Particulate Matter in the Eastern United States and Effectiveness of Emission Control Programs.” *Science of The Total Environment* 490 (August): 171–81. https://doi.org/10.1016/j.scitotenv.2014.04.064.

Zieliński, T. 2004. “Studies of Aerosol Physical Properties in Coastal Areas.” *Aerosol Science and Technology* 38 (5): 513–24. https://doi.org/10.1080/02786820490466738.